https://doi.org/10.5194/essd-2023-239
Preprint. Discussion started: 28 September 2023

Open Access Earth System Science Data Discussions

A decade-long cruise time-series (2008–2018) of physical and biogeochemical conditions in the southern Salish Sea, North America

Simone R. Alin[1], Jan A. Newton[2,3], Richard A. Feely[1], Dana Greeley[1], Beth Curry[2,4], Julian Herndon[5], and Mark Warner[3]

[1] Pacific Marine Environmental Laboratory, National Oceanic and Atmospheric Administration, 7600 Sand Point Way NE, Seattle, Washington 98115, USA
[2] Applied Physics Laboratory, University of Washington, Box 355640, Seattle, Washington 98105, USA
[3] School of Oceanography, University of Washington, 1492 NE Boat St., Seattle, Washington 98105, USA
[4] Currently at: MRV Systems, LLC, 6165 Greenwich Dr., San Diego, California 92122, USA
[5] Cooperative Institute for Climate, Ocean, and Ecosystem Studies, University of Washington, 3737 Brooklyn Ave NE, Seattle, Washington 98105, USA

ORCID IDs
Alin: 0000-0002-8283-1910
Newton: 0000-0002-2551-1830
Feely: 0000-0003-3245-3568
Greeley: 0000-0003-4356-5899
Curry: 0000-0002-6534-4475
Herndon: 0009-0001-9820-9026
Warner: 0000-0001-7678-441X

***Correspondence to*: Simone R. Alin (simone.r.alin@noaa.gov)**

Abstract. Coastal and estuarine waters of the northern California Current System and southern Salish Sea host an observational network capable of characterizing biogeochemical dynamics related to ocean acidification, hypoxia, and marine heatwaves. Here we compiled data sets from a set of cruises conducted in estuarine waters of Puget Sound (southern Salish Sea) and its boundary waters (Strait of Juan de Fuca and Washington coast). This data product provides data from a decade of cruises with consistent formatting, extended data quality control, and multiple units for parameters such as oxygen with different end use needs and conventions. All cruises obtained high-quality temperature, salinity, inorganic carbon, nutrient, and oxygen observations to provide insight into the dynamic distribution of physical and biogeochemical conditions in this large urban estuary complex on the west coast of North America. At all sampling stations, CTD casts included sensors for measuring temperature, conductivity, pressure, and oxygen concentrations. Laboratory analyses of discrete water samples collected at all stations throughout the water column in Niskin bottles provided measurements of dissolved inorganic carbon (DIC), dissolved oxygen, nutrient (nitrate, nitrite, ammonium, phosphate, silicate), and total alkalinity (TA) content. This data product includes observations from 35 research cruises, including 715 oceanographic profiles, with >7490 sensor measurements of temperature, salinity, and oxygen; ≥6070 measurements of discrete oxygen and nutrient samples; and ≥4462 measurements of inorganic carbon variables (i.e., DIC and TA). The observations comprising this cruise compilation collectively characterize the spatial and temporal variability of a region with large dynamic ranges of the physical (temperature = 6.0–21.8 °C, salinity = 15.6–34.0) and biogeochemical parameters (oxygen = 12–481 µmol kg^{-1}, dissolved inorganic carbon = 1074–2362 µmol kg^{-1}, total alkalinity = 1274–2296 µmol kg^{-1}) central to understanding ocean acidification and hypoxia in this productive estuary system with numerous interacting human impacts on its ecosystems. All observations conform to the climate-quality observing guidelines of the Global Ocean Acidification Observing Network, the U.S. National Oceanic and Atmospheric Administration's Ocean Acidification Program, and ocean carbon

https://doi.org/10.5194/essd-2023-239
Preprint. Discussion started: 28 September 2023

community best practices. This on-going cruise time-series supports the estuarine and coastal monitoring and research objectives of the Washington Ocean Acidification Center and U.S. National Oceanic and Atmospheric Administration (NOAA) Ocean and Atmospheric Research programs, and provides diverse end users information needed to frame biological impacts research, validate numerical models, inform state and tribal water quality and fisheries management, and support decision makers. All 2008–2018 cruise time-series measurements used in this publication are available at https://doi.org/10.25921/zgk5-ep63 (Alin et al., 2022).

1 Introduction

Estuaries are productive environments that serve as breeding grounds for ecologically and economically important finfish and shellfish species. Estuarine ecosystems are particularly vulnerable to ocean acidification as a result of the overlap of global oceanic processes bringing anthropogenic carbon dioxide (CO_2) into estuary environments that are already high in CO_2 due to a combination of natural and anthropogenic local processes (Feely et al., 2010; Wallace et al., 2014; Pacella et al., 2018; Cai et al., 2021; Windham-Myers et al., 2018; Bednaršek et al., 2020a; Alin et al., 2023b). Rivers transport terrestrial runoff high in nutrients, oxygen, and carbon dioxide into estuarine surface waters from forested, agricultural, and urban landscapes (Evans et al., 2013; Hales et al., 2017; Voss et al., 2014; Johannessen et al., 2003, 2015; Barnes and Raymond, 2009; Windham-Myers et al., 2018; Moore et al., 2017; Hunt et al., 2023). In contrast, marine source waters entering Northeast Pacific estuarine ecosystems are naturally low in oxygen (O_2) and high in dissolved inorganic carbon (DIC) content due to global thermohaline circulation and coastal upwelling of subsurface water masses previously isolated from the atmosphere for decades (Feely et al., 2004, 2010, 2016; Sabine et al., 2004) (Feely et al. 2004, 2010, 2016; Sabine et al. 2004). Thus, estuaries receive naturally acidified from both riverine inputs and subsurface marine source waters, particularly along coastal upwelling systems and in the NE Pacific.

Carbonate system observations in coastal and estuarine NE Pacific ecosystems have proliferated over the past decade, including water column discrete measurements of dissolved inorganic carbon (DIC), total alkalinity (TA), pH (on the total scale, pH_T), and carbonate ion content ($[CO_3^{2-}]$) and surface CO_2 partial pressure or fugacity (pCO_2 or fCO_2) and pH_T from moored and underway sensor systems (e.g., Feely et al., 2010, 2016; Ianson et al., 2016; Sutton et al., 2016; Fassbender et al., 2018). Surface ocean CO_2 and pH observations from estuarine and coastal regions are incorporated into the Surface Ocean CO_2 Atlas for annual data releases (Bakker et al., 2016), and provide regional end users with annual updates on the status of pCO_2 in Washington's marine surface waters (Alin et al. sections in PSEMP Marine Waters Workgroup, 2022). Recently North American climate-quality coastal cruise biogeochemical data sets were compiled and quality controlled to create an internally consistent coastal data product for inorganic carbon, oxygen, and nutrients called Coastal Ocean Data Analysis Product in North America (CODAP-NA, Jiang et al., 2021). While the CODAP-NA workflow addresses many of the challenges of working with coastal oceanographic data—e.g., working with data from highly dynamic environments and data streams of variable uncertainties—the Jiang et al. (2021) data product did not incorporate estuarine data sets, as these challenges can be even more profound with estuarine observational data sets. Both high-resolution surface observations and depth-resolved but less frequent cruise observations of biogeochemistry are critical for assessing the on-going acidification of coastal and estuarine environments and its impacts on ecological and human communities, as well as the response of biogeochemistry to other aspects of climate change such as marine heatwaves and other extreme events (e.g., Alin et al., 2023b).

Here, we describe a decade-long (2008–2018) time-series of observations from 35 cruises conducted in estuarine waters of Puget Sound and its boundary waters that provides synoptic snapshots of conditions in Washington's estuarine and coastal waters during

https://doi.org/10.5194/essd-2023-239
Preprint. Discussion started: 28 September 2023

all seasons and spanning a wide range of weather and climate conditions from 2008 to 2018. The compiled Salish cruise data product includes high-quality physical, inorganic carbon, nutrient, and oxygen measurements collected throughout the water column. We focus here on briefly describing the core parameters measured on the cruises, with particular emphasis on the variables needed to calculate all other components of the carbonate system (i.e., temperature, salinity, and dissolved inorganic carbon (DIC), total alkalinity (TA), phosphate, and silicate content). We also provide nitrate, nitrite, and ammonium observations for their importance in driving primary production or reflecting anomalous redox conditions in this estuary. In a companion paper, we delve into the seasonal variability of temperature, salinity, oxygen, and the calculated ocean acidification parameters, fCO_2 and aragonite saturation state (Ω_{arag}), as well as the relative frequency and severity of acidified, hypoxic, and thermal conditions crossing thresholds of regionally important species during a seasonally resolved subset of this time-series (Alin et al., 2023b). All observations described herein conform to analytical standards described in the ocean carbon community best practices guide (Dickson et al., 2007). These measurements also meet climate-quality monitoring guidelines of the Global Ocean Acidification Observing Network, which requires provision of individual measurement uncertainty and the determination of two core inorganic carbon system parameters and all ancillary parameters needed for full carbonate system constraint (Newton et al., 2015).

2 Data collection, quality assurance, and initial quality control

Puget Sound (PS) is a glacial fjord estuary complex on the North American Pacific coast, receiving drainage from forested, agricultural, and urban landscapes. It comprises the southernmost part of the Salish Sea, which also encompasses the Strait of Juan de Fuca and the Strait of Georgia (Figure 1). Puget Sound is comprised of four basins—Main Basin, South Sound, Whidbey Basin, and Hood Canal—as well as Admiralty Reach, a glacial sill complex defining the entrance to Puget Sound. We refer to the most ocean-influenced areas, the coast and Strait of Juan de Fuca, collectively as "boundary" waters for Puget Sound. The Strait of Juan de Fuca (SJdF), Admiralty Reach (AR), Main Basin (MB), and South Sound (SS) have well-mixed waters due to tidal and wind mixing within the basins. In contrast, Whidbey Basin (WB) and Hood Canal (HC) are narrower, and vertical mixing is inhibited by large river inputs that result in strong stratification.

The February 2008–October 2018 cruises described here are part of an on-going Salish cruise time-series, consisting of Sound-to-Sea (S2S) and Puget Sound (PS) cruises (Table 1; Alin et al., 2022) surveying physical and biogeochemical conditions throughout the water column. Semi-annual S2S cruises sample a transect of stations between Seattle and the coastal ocean acidification mooring “Ćhá?ba·” offshore from La Push, Washington. Seasonal PS cruises sample stations in all sub-basins of the Puget Sound, with consistent timing in April, July, and September since 2014. Of the 35 cruises, 12 occupied S2S stations, 17 surveyed Puget Sound, four sampled only at Ćhá?ba·, and two cruises occupied both S2S and PS stations (Figure 1). Surveys started during all months of the year, except June and December, with the most frequent months being April (n = 5), May (5), July (5), September (7), and October (6), and one each in February, August, and November (Table 1). S2S cruises provided the opportunity to sample stations between the Main Basin of Puget Sound and coastal Washington waters adjacent to the Ćhá?ba· mooring, including the Strait of Juan de Fuca, and occurred most frequently in May (5) and October (5), providing early and late upwelling season snapshots in boundary waters. Puget Sound cruises have occurred most frequently in April (n = 4), July (5), and September (6). The resulting cruise data set comprises 3693 samples with paired observations of inorganic carbon, nutrients, oxygen, and CTD measurements across a complex estuary system and along the gradient from the estuary to the coastal ocean, and up to 7525

https://doi.org/10.5194/essd-2023-239
Preprint. Discussion started: 28 September 2023

observations lacking one or more measurements (Table 2). In this paper, we describe the methods used to produce all data in the corresponding data product.

The Salish cruises described here were preceded by semi-annual Puget Sound Regional Synthesis Model (PRISM) cruises that occupied the same Puget Sound stations, typically in June and December, but the 1998–2007 PRISM cruises had not yet initiated inorganic carbon measurements and were thus not included in this data compilation and description (PRISM data are available at: https://nvs.nanoos.org/CruiseSalish). The seasonal Salish cruises (2014–2018) included in this data product and further described in Alin et al. (2023b) are ongoing, and updates to this cruise time-series will be provided in follow-on papers and data products.

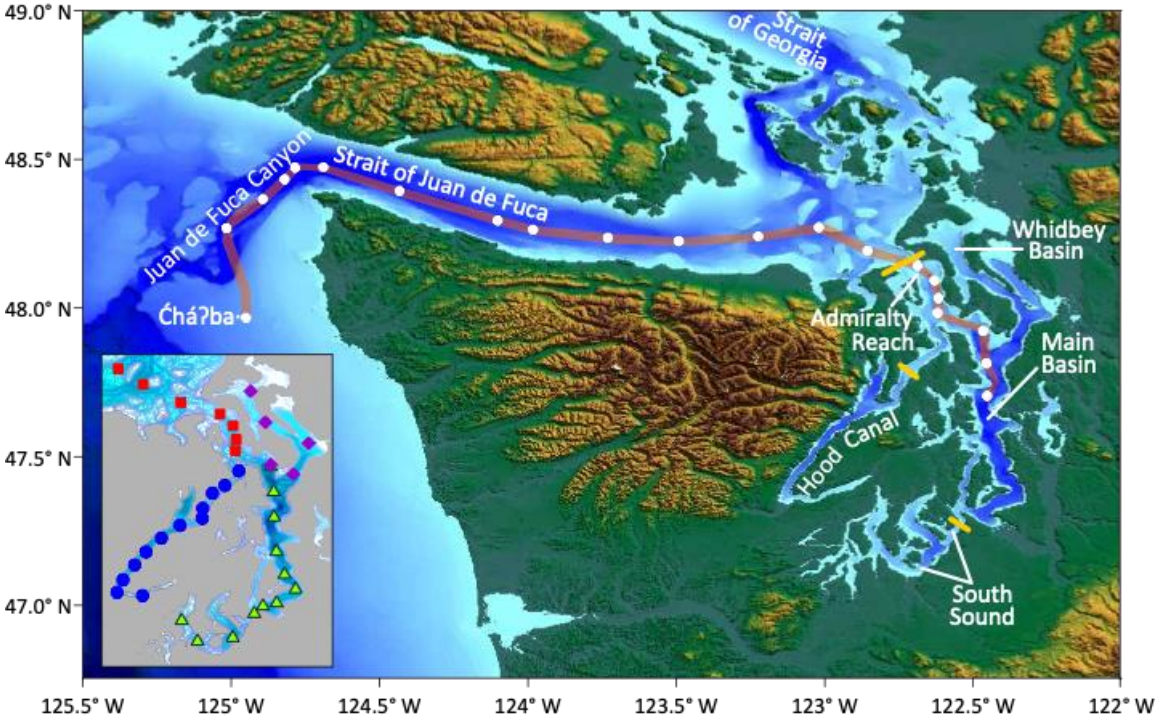

Figure 1: Map of the southern Salish Sea and its boundary waters with all study basins named. The subset of sampling stations tracing a path between the Ćhá?ba· mooring on the Washington state (USA) continental shelf to the Main Basin of Puget Sound constitute the Sound-to-Sea (S2S) transects. Inset map shows station groupings used for analyses of Puget Sound cruises: Admiralty Reach (AR, red squares), Main Basin–South Sound (MB–SS, green triangles), Whidbey Basin (WB, purple diamonds), and Hood Canal (HC, blue circles). Yellow dashes in the main figure denote locations of glacial sills. Topographic and bathymetric data were extracted from the NOAA National Centers for Environmental Information Grid Extract Coastal Relief Model (3-second resolution, https://www.ncei.noaa.gov/maps/grid-extract/, accessed Nov. 13, 2014). Data were gridded in *Surfer* using a minimum curve gridding technique.

https://doi.org/10.5194/essd-2023-239
Preprint. Discussion started: 28 September 2023

Open Access Earth System Science Data Discussions

Table 1. Details of each cruise included in the 2008–2018 Salish cruise data product including cruise identification (ID), dates, contributing research programs, geographic scope of observations, ship, and funding sources.

Cruise ID	Dates	Research programs[a]	Geographic scope[b]	Ship	Funding sources[c]
TN216	February 4–8, 2008	PRISM, PMEL-CO_2	Puget Sound	R/V *Thomas G. Thompson*	PRISM, PMEL
BOLD085	August 11–15, 2008	EPA, PRISM, PMEL-CO_2	Puget Sound and Sound-to-Sea	EPA Ocean Survey Vessel *Bold*	EPA, PRISM, PMEL
RBTSN200909	September 29–October 2, 2009	PRISM, PMEL-CO_2	Puget Sound	R/V *Jack Robertson*	PRISM, PMEL
TN256	October 31–November 3, 2010	PRISM, PMEL-CO_2	Puget Sound	R/V *Thomas G. Thompson*	PRISM, PMEL
TN264	May 22, 2011	PRISM, PMEL-CO_2	Ćhá?ba· only	R/V *Thomas G. Thompson*	SOO, PRISM, PMEL
TN267	August 8, 2011	PRISM, PMEL-CO_2	Ćhá?ba· only	R/V *Thomas G. Thompson*	SOO, PRISM, PMEL
TN270	October 8–14, 2011	PRISM, PMEL-CO_2	Puget Sound and Sound-to-Sea	R/V *Thomas G. Thompson*	PRISM, PMEL
TN281	May 25–26, 2012	PRISM, PMEL-CO_2	Sound-to-Sea (partial)	R/V *Thomas G. Thompson*	SOO, PRISM, PMEL
TN290B	January 17, 2013	PRISM, PMEL-CO_2	Ćhá?ba· only	R/V *Thomas G. Thompson*	SOO, PRISM, PMEL
TN296	April 22–23, 2013	UW, NANOOS, PMEL-CO_2	Sound-to-Sea (partial)	R/V *Thomas G. Thompson*	SOO, PRISM, PMEL
TN301	September 22–25, 2013	UW, NANOOS, PMEL-CO_2	Sound-to-Sea	R/V *Thomas G. Thompson*	SOO, WOAC, PMEL
CAB1019	July 14–18, 2014	WOAC, PMEL-CO_2	Puget Sound	R/V *Clifford A. Barnes*	WOAC, PMEL
CAB1023	September 29–October 3, 2014	WOAC, PMEL-CO_2	Puget Sound	R/V *Clifford A. Barnes*	WOAC, PMEL
TN315	October 22–31, 2014	UW, PMEL-CO_2	Sound-to-Sea	R/V *Thomas G. Thompson*	SOO, WOAC, PMEL
CAB1028	April 5–9, 2015	WOAC, PMEL-CO_2	Puget Sound	R/V *Clifford A. Barnes*	WOAC, PMEL
TN322	May 23–24, 2015	UW, PMEL-CO_2	Sound-to-Sea	R/V *Thomas G. Thompson*	SOO, WOAC, PMEL
CAB1034	July 7–11, 2015	WOAC, PMEL-CO_2	Puget Sound	R/V *Clifford A. Barnes*	WOAC, PMEL
CAB1037	September 23–27, 2015	WOAC, PMEL	Puget Sound	R/V *Clifford A. Barnes*	WOAC, PMEL
TN333	November 16–19, 2015	UW, PMEL-CO_2	Sound-to-Sea	R/V *Thomas G. Thompson*	SOO, WOAC, PMEL
SH1604	March 17–19, 2016	NANOOS, PMEL-CO_2	Sound-to-Sea	NOAA Ship *Bell M. Shimada*	OAP, OMAO, WOAC, PMEL
CAB1041	April 5–9, 2016	WOAC, PMEL-CO_2	Puget Sound	R/V *Clifford A. Barnes*	SOO for WOAC, WOAC, PMEL
TN343	May 23–24, 2016	NANOOS, PMEL-CO_2	Ćhá?ba· only	R/V *Thomas G. Thompson*	WOAC, PMEL
CAB1045	July 7, 2016 and July 21–25, 2016	WOAC, PMEL-CO_2	Puget Sound	R/V *Clifford A. Barnes*	WOAC, PMEL
CAB1050	September 21–25, 2016	WOAC, PMEL-CO_2	Puget Sound	R/V *Clifford A. Barnes*	SOO for WOAC, WOAC, PMEL
AQ201610	October 24–27, 2016	NANOOS, WOAC, PMEL-CO_2	Sound-to-Sea	F/V *Aquila*	OAP, OMAO, WOAC, PMEL

https://doi.org/10.5194/essd-2023-239
Preprint. Discussion started: 28 September 2023

CAB1065	April 4–10, 2017	WOAC, PMEL-CO_2	Puget Sound	R/V *Clifford A. Barnes*	WOAC, PMEL
RBTSN201705	May 2–5, 2017	WOAC, PMEL-CO_2	Sound-to-Sea	R/V *Jack Robertson*	WOAC, PMEL
CAB1075	July 11–15, 2017	WOAC, PMEL-CO_2	Puget Sound	R/V *Clifford A. Barnes*	WOAC, PMEL
CAB1079	September 11–15, 2017	WOAC, PMEL-CO_2	Puget Sound	R/V *Clifford A. Barnes*	WOAC, PMEL
AQ201710	October 16–18, 2017	WOAC, PMEL-CO_2	Sound-to-Sea	F/V *Aquila*	OAP, OMAO, WOAC, PMEL
RC001	April 7–11, 2018	WOAC, PMEL-CO_2	Puget Sound	R/V *Rachel Carson*	WOAC, PMEL
RBTSN201805	May 23–24, 2018	WOAC, PMEL-CO_2	Sound-to-Sea	R/V *Jack Robertson*	WOAC, PMEL
RC006	July 23–27, 2018	WOAC, PMEL-CO_2	Puget Sound	R/V *Rachel Carson*	WOAC, PMEL
RC007	September 11–15, 2018	WOAC, PMEL-CO_2	Puget Sound	R/V *Rachel Carson*	WOAC, PMEL
NORSEMANIIOCT18	October 16–19, 2018	WOAC, PMEL-CO_2	Sound-to-Sea	R/V *Norseman II*	WOAC, PMEL

[a] Research programs are those institutional programs that led the collection of the core variables described in this publication of each cruise data set. [b] Geographic scope refers to the area within Washington State marine waters that was sampled on each cruise and refers to station groupings described in Figure 1. [c] Funding programs provided support for ship time and principal investigator, cruise participant, and laboratory or data analyst salaries. Abbreviations for research and funding programs are: WOAC = Washington Ocean Acidification Center, UW = University of Washington, EPA = U.S. Environmental Protection Agency, NOAA = U.S. National Oceanic and Atmospheric Administration, PMEL = NOAA Pacific Marine Environmental Laboratory, PMEL-CO_2 = PMEL CO_2 Research Group, PRISM = UW Puget Sound Regional Synthesis Model, SOO = UW School of Oceanography, NANOOS = Northwest Association of Networked Ocean Observing Systems, OAP = NOAA Ocean Acidification Program, OMAO = NOAA Office of Marine and Aviation Operations.

Table 2. Final data variable names, descriptions, units, and measurement temperature (T) and pressure (P) conditions for observations in the Salish cruise data product.

Variable name	Description	Units	Measurement T and P conditions[c]
CRUISE_ID	Cruise identification (ID) as shown in Table 1, normally a code assigned by each ship	character string	
STATION_ID	CTD station number corresponding to PRISM station numbers, the usual P preceding the number has been deleted[a]	integer	
LONGITUDE_DEC	Longitude of CTD station	decimal degrees	
LATITUDE_DEC	Latitude of CTD station	decimal degrees	
NISKIN_NO	Number of Niskin bottle discrete samples drawn from	integer	
MONTH_UTC	Calendar month of measurement or sample collection in Coordinated Universal Time (UTC)	M	
DAY_UTC	Calendar day of measurement or sample collection in UTC	D	
YEAR_UTC	Calendar year of measurement or sample collection in UTC	YYYY	
TIME_UTC	Time of measurement or sample collection in UTC	HH:MM:SS	
CTDPRS_DBAR	Hydrostatic pressure recorded from CTD at the depth where the sample is taken[a]	decibars (db)	In situ
CTDTMP_ITS90_DEG_C	Temperature recorded from CTD at the sampling depth, on the ITS-90 scale [b]	°C	In situ
CTDSAL_PSS78	Practical salinity calculated from conductivity recorded by CTD at the sampling depth, on the Practical Salinity Scale (PSS-78)[b]	unitless	In situ
SIGMATHETA_KG_M3	Potential density anomaly, also known as sigma theta, referenced to 0 db pressure[b]	kg m^{-3}	In situ

https://doi.org/10.5194/essd-2023-239
Preprint. Discussion started: 28 September 2023

CTDOXY_MG_L	Dissolved oxygen measured by oxygen sensors mounted on the CTD[b]	mg L^{-1}	In situ
CTDOXY_FLAG_W	Quality control flag associated with CTD sensor oxygen measurement	WOCE flags[e]	
OXYGEN_MG_L_#	Dissolved oxygen measured from discrete bottle samples by Winkler analysis[d]	mg L^{-1}	Laboratory
OXYGEN_FLAG_W	Quality control flag associated with bottle oxygen measurement	WOCE flags[e]	
CTDOXY_UMOL_KG_ADJ	Dissolved oxygen concentration measured by CTD sensors and adjusted for an offset from bottle oxygen values	µmol kg^{-1}	In situ
RECOMMENDED_OXYGEN_UMOL_KG	Dissolved oxygen Winkler measurements of "acceptable" quality, with adjusted CTDOXY measurements replacing missing values	µmol kg^{-1}	Laboratory for Winkler, in situ for CTD data
RECOMMENDED_OXYGEN_MG_L	Dissolved oxygen Winkler measurements of "acceptable" quality, with adjusted CTDOXY measurements replacing missing values	mg L^{-1}	Laboratory for Winkler, in situ for CTD data
RECOMMENDED_OXYGEN_ML_L	Dissolved oxygen Winkler measurements of "acceptable" quality, with adjusted CTDOXY measurements replacing missing values	mL L^{-1}	Laboratory for Winkler, in situ for CTD data
PHOSPHATE_UMOL_L	Concentration of phosphate (PO_4^{3-}) measured from discrete bottles	µmol L^{-1}	Laboratory
SILICATE_UMOL_L	Concentration of silicate (orthosilicic acid, $Si(OH)_4$) measured from discrete bottles, laboratory[c]	µmol L^{-1}	Laboratory
NITRATE_UMOL_L	Concentration of nitrate (NO_3^-) measured from discrete bottles	µmol L^{-1}	Laboratory
NITRITE_UMOL_L	Concentration of nitrite (NO_2^-) measured from discrete bottles	µmol L^{-1}	Laboratory
AMMONIUM_UMOL_L	Concentration of ammonium (NH_4^+) measured from discrete bottles	µmol L^{-1}	Laboratory
PHOSPHATE_UMOL_KG	Concentration of phosphate (PO_4^{3-}) measured from discrete bottles	µmol kg^{-1}	Laboratory
SILICATE_UMOL_KG	Concentration of silicate (orthosilicic acid, $Si(OH)_4$) measured from discrete bottles	µmol kg^{-1}	Laboratory
NITRATE_UMOL_KG	Concentration of nitrate (NO_3^-) measured from discrete bottles	µmol kg^{-1}	Laboratory
NITRITE_UMOL_KG	Concentration of nitrite (NO_2^-) measured from discrete bottles	µmol kg^{-1}	Laboratory
AMMONIUM_UMOL_KG	Concentration of ammonium (NH_4^+) measured from discrete bottles	µmol kg^{-1}	Laboratory
NUTRIENTS_FLAG_W	Quality control flag associated with nutrient laboratory measurement	WOCE flags[e]	
DIC_UMOL_KG	Concentration of dissolved inorganic carbon measured from discrete bottles[d]	µmol kg^{-1}	Laboratory
DIC_FLAG_W	Quality control flag associated with DIC laboratory measurement	WOCE flags[e]	
TA UMOL_KG	Total alkalinity measured from discrete bottles[d]	µmol kg^{-1}	Laboratory
TA_FLAG_W	Quality control flag associated with TA laboratory measurement	WOCE flags[e]	

[a] See http://nvs.nanoos.org/CruiseSalish for full information on locations and descriptive names for each station. [b] Measurements taken on CTD upcast at the same depth where the Niskin bottle associated with a discrete bottle measurement was closed. [c] Designations "in situ" and "laboratory" denote the temperature and pressure conditions under which each measurement was taken. [d] In the submitted data product, Winkler oxygen measurements have some replicate samples, and the replicate number will thus be inserted in place of the # sign, e.g. "OXYGEN_MG_L_1", "OXYGEN_MG_L_2", etc. [e] World Ocean Circulation Experiment (WOCE) water sample quality flag definitions are used: 2 = acceptable value, 3 = questionable value, 4 = bad value, 5 = value not reported, 6 = mean of replicate measurements (used for DIC_UMOL_KG and TA_UMOL_KG only), 9 = sample not drawn (Tables 4.9 and 4.10 in WOCE, 1998 for bottle and CTD data, respectively).

https://doi.org/10.5194/essd-2023-239
Preprint. Discussion started: 28 September 2023

2.1 CTD profiles and water collection

On all cruises, we surveyed the network of either the S2S or PS sampling stations using Niskin bottles and CTD (conductivity-temperature-depth), oxygen, and additional sensors affixed to a rosette cage and deployed from a research vessel through the water column (Table 1). Downcast CTD sensor profiles were collected at each sampling station using a Sea Bird 911plus CTD plus deck box combination (except where noted in individual cruise metadata), allowing sensor data to be seen in real-time. Upcast CTD data, corresponding to when the Niskin bottles on the rosette cage were fired and water samples were collected, are the focus of this publication and the corresponding data package (Alin et al., 2022). The conductivity, temperature, and pressure sensor initial accuracy errors are ±0.0003 S m^{-1}, ±0.001 °C, and ±0.015% of the full-scale range, respectively; with typical stability on the order of 0.0003 S m^{-1} per month, 0.0002 °C per month, and 0.02% of full scale per year; and master clock error contributions of 0.00005 S m^{-1}, 0.00016° C, and 0.3 dbar. CTD sensor data were processed using Sea Bird's proprietary data processing software using the Data Conversion and Bottle Summary modules, which convert raw data from the CTD to engineering units, derive dependent variables (namely, salinity and potential density anomaly, or sigma theta, σ_θ), and write a bottle data summary to an output file. Temperatures were submitted on the International Temperature Scale of 1990 (ITS-90). Salinities in this data product were submitted on the Practical Salinity Scale (PSS-78), which is a unitless quantity but some practitioners incorrectly express it as PSU to designate that it uses this scale (IOC, SCOR, and IAPSO, 2010).

2.2 Dissolved oxygen

Dissolved oxygen concentration was measured both by Sea Bird oxygen (SBE43) sensors attached to the CTD and by Winkler analyses of discrete bottle samples collected from the Niskins and analyzed by University of Washington staff. The SBE43 initial accuracy is ±2% of saturation, with typical stability of 0.5% per 1000 hours of deployed time.

Discrete oxygen samples were always collected first from a Niskin bottle after opening it, due to the rapid air-sea gas exchange of oxygen. To collect discrete dissolved oxygen samples, a Tygon tube was attached to the Niskin bottle and flushed so no air remained. A 125-mL iodine flask was inverted over the upward-pointing tube and flushed, rinsing and reverting the bottle to allow it to fill, overflowing three times its volume. The tube was withdrawn without turbulence, maintaining an overfull bottle. Reagents were prepared and added to samples as described in IOC and SCOR (1994). The flask was capped without introducing a bubble and inverted about a dozen times to mix thoroughly. The bottle was allowed to settle, then remixed, and a bead of deionized water added to the lid for an airtight seal. We collected and analyzed replicate samples from approximately 10% of the Niskins sampled.

The analysis method is based upon whole-flask titration of iodine (Carpenter, 1965; as described by Codispoti, 1988), which is produced by an equivalent amount of dissolved oxygen. The nominally 125-mL iodine flasks used for sampling were pre-calibrated so their volumes were precisely known. Samples were titrated within a day or two of being collected, allowing the samples to come to room temperature where the titration occurred. Discrete oxygen samples were used to validate sensor O_2 observations on the CTD package. Precision of 1% on Winkler oxygen measurements was calculated as the average standard error on triplicate analyses.

https://doi.org/10.5194/essd-2023-239
Preprint. Discussion started: 28 September 2023

2.3 Dissolved inorganic carbon

Inorganic carbon samples were collected from Niskins immediately after oxygen samples and analyzed at NOAA Pacific Marine Environmental Laboratory (NOAA/PMEL). An exception to sampling order was on the August 2008 cruise, when spectrophotometric pH (on the total scale, pH_T) samples were collected between O_2 and DIC samples; however, these directly measured pH_T data are not included in this data product. A combined sample for dissolved inorganic carbon (DIC) and total alkalinity (TA) measurements was drawn into ~540-mL borosilicate glass flasks using silicone tubing according to procedures outlined in the *Guide to Best Practices for Ocean CO_2 Measurements* (SOP 1, Dickson et al., 2007). Briefly, flasks were rinsed once and filled from the bottom with care not to entrain any bubbles, overflowing by at least one-half volume. The sample tube was pinched and withdrawn, creating a small headspace, and 0.2 mL of saturated mercuric chloride ($HgCl_2$) solution was added as a preservative. Sample bottles were then sealed with glass stoppers lightly covered with Apiezon-L grease. Stoppers were held in place until analysis with a thick rubber band over the stopper attached to a plastic clamp around the neck of the sample flask. Sample bottles were inverted several times to ensure mixing of the $HgCl_2$ throughout the sample. DIC samples were collected from a variety of depths, with approximately 5% of samples drawn in duplicate (or occasionally triplicate). All samples were stored under cool, dark conditions until analysis.

DIC concentrations were measured at PMEL on analytical systems consisting of a coulometer (UIC Inc.) coupled with a Single Operator Multiparameter Metabolic Analyzer (SOMMA) developed to extract DIC from seawater (Johnson et al., 1985, 1987, 1993; Johnson, 1992). Each coulometer was calibrated at the beginning of each analysis day, when a fresh coulometric cell was prepared, by injecting aliquots of pure CO_2 (99.999%) by way of an eight-port valve (Wilke et al., 1993) outfitted with two calibrated sample loops of different sizes (~1 mL and ~2 mL). Calibration consisted of running one or more sets of gas loop injections at the beginning of each cell. Typically, 20–25 samples were analyzed per coulometric cell.

The accuracy of SOMMA measurements was determined with the use of Certified Reference Materials (CRMs), consisting of filtered and UV-irradiated seawater and supplied by the laboratory of Professor Andrew Dickson of Scripps Institution of Oceanography (SIO). Certified reference values of CRMs were determined manometrically on land at SIO. CRMs were measured near the beginning of each cell. Replicate samples were typically run throughout the life of the cell solution for quality assurance and to assess the integrity of the coulometer cell solutions. All DIC data have been corrected for dilution by the small amount of saturated $HgCl_2$ added and for observed offsets between PMEL measurements and certified CRM batch values. An estimate of precision is provided by the replicate samples collected from approximately 5% of the Niskins sampled. The average absolute difference from the mean among replicates is typically on the order of 1.5 µmol kg^{-1}. This is consistent with our independent measurements of accuracy of the CRMs using the gas calibration loops. No systematic differences among replicates were observed, except in near-surface waters, where stratification is sufficiently strong in Puget Sound that a pair of samples collected in immediate succession from the same Niskin can have DIC (and TA) values >50 µmol kg^{-1} apart from each other. Thus, near-surface replicate samples were not used to estimate analytical precision.

2.4 Total alkalinity

After DIC measurement on a sample, the remaining seawater in a sample bottle was analyzed at NOAA/PMEL to determine TA by acidimetric titration. The method is based upon the open-cell method described by Dickson et al. (2003, SOP 3b, 2007), wherein the sample is first acidified to reduce sample pH to less than 3.6, followed by bubbling CO_2-free air through the sample to facilitate removal of the CO_2 evolved by the acid addition. After removal of all carbonate species from solution, the titration proceeds until

https://doi.org/10.5194/essd-2023-239
Preprint. Discussion started: 28 September 2023

a pH of less than 3.0 is attained. Then the equivalence point is evaluated from titration points in the pH region 3.0–3.5 using a non-linear, least-squares procedure that corrects for reactions with sulfate and fluoride ions (Dickson et al., 2003). Titration progress is monitored by measuring the electromotive force of a combination glass-reference electrode. Instrument control and data acquisition occur via custom software developed by Professor Andrew Dickson's laboratory at SIO. Typical titrations were completed in 10–14 minutes and required 20–24 acid additions to reach a pH of 3.0.

Titrations were carried out in water-jacketed, 250-mL beakers to ensure temperature stability. The temperature of the samples and the beakers was controlled by use of a refrigerated recirculating water bath. Seawater samples were measured gravimetrically (105–135 g depending on salinity) to ensure a sufficient number of titration points were achieved (typically 18–22). A Metrohm Dosimat 765 was used to deliver certified acid titrant to the sample beaker in small, precise increments (0.04–0.05 mL depending on sample size and salinity). The acid titrant used was 0.1 mol kg^{-1} hydrochloric acid prepared in 0.6 mol kg^{-1} sodium chloride to approximate the ionic strength of seawater (0.7 mol kg^{-1}). The titrant was coulometrically analyzed and certified by Prof. Andrew Dickson's laboratory.

Analytical accuracy was assessed by periodic analysis of the same CRMs as used for DIC. No corrections were made for offsets between the certified and measured CRM values when the offset was below 2 µmol kg^{-1}, the difference from accepted and measured CRM values was added or subtracted from measured sample values for offsets between 2 and 4 µmol kg^{-1}, and above 4 µmol kg^{-1}, instruments were not run until repaired. Precision was monitored by analysing replicates drawn from approximately 10% of the Niskins sampled.

2.5 Nutrients

One bottle sample for nutrients was collected from each Niskin after oxygen and inorganic carbon bottle samples had been collected, for subsequent analysis of phosphate, silicate, nitrate, nitrite, and ammonium concentrations at the Marine Chemistry Laboratory at the University of Washington (UW) School of Oceanography. To collect samples, a 60-mL HDPE syringe was prepared by removing the plunger and attaching a Nalgene filter (surfactant-free cellulose, 25 mm, 0.45-micron pore size). The plunger and the inside of the syringe were rinsed three times using seawater from the Niskin bottle. The syringe was then filled with sample water from the Niskin, and the plunger inserted. About 1 mL of sample water was filtered through the filter, then about 5–10 mL of sample was dispensed into the 60-mL HDPE sample bottle to rinse the bottle and cap, with the rinse water then discarded. Rinsing was repeated three times. Then about 45 mL of sample was filtered into the sample bottle, such that it was ~2/3 full. The cap was secured and the bottle frozen upright until analyzed.

Analyses and calibration followed the protocols of the World Ocean Circulation Experiment (WOCE) Hydrographic Program (IOC and SCOR, 1994) using a Seal Analytical AA3 in the UW Marine Chemistry Laboratory (accreditation codes can be seen at: University of Washington, 2021). Minimum detection limits were 0.04 µM for phosphate, 0.23 µM for silicate, 0.29 µM for nitrate, 0.01 µM for nitrite, and 0.05 µM for ammonium.

2.6 Uncertainty of oceanographic measurements

Overall temperature and salinity uncertainties are ±0.01 °C and ±0.02, respectively. Oxygen measurement uncertainties were ±2% of saturation on CTD oxygen measurements and precision of 1% on Winkler oxygen measurements. Measurement uncertainties were ±0.1% (~2 µmol kg^{-1}) on DIC and TA measurements. Uncertainty on nutrient measurements were ±2%. However, it should

https://doi.org/10.5194/essd-2023-239
Preprint. Discussion started: 28 September 2023

be noted that the uncertainties given above reflect analytical uncertainties for discrete biogeochemical measurements (Winkler O_2, DIC, TA, and nutrient analyses) but cannot capture the uncertainty associated with field sampling or sample handling errors (e.g., Niskins firing at the wrong depth or samples incorrectly preserved or stored).

3 Unit conversions and data quality control

All unit conversions and extended primary QC measures are described in this section. All measurements were subjected to quality assurance measures in the laboratory as described in section 2, as well as quality control measures immediately following analysis, which reflect instrument diagnostic information and other observations of measurement quality and sample integrity made in the laboratory. Initial quality control (QC) flags were assigned on the basis of laboratory instrument diagnostics only for DIC and TA analyses based on WOCE water sample quality flag definitions listed in the footnotes to Table 1. Here we describe calculations undertaken to convert units to prepare for subsequent analyses of derived inorganic carbonate system parameters necessary for understanding ocean acidification, such as calcium carbonate saturation states (Ω), pH_T, partial pressure or fugacity of CO_2, and Revelle Factor, using CO2SYS (e.g., Lewis and Wallace, 1988; van Heuven et al., 2011; Pelletier et al., 2007), the R package *seacarb* (Gattuso et al., 2022), or other water chemistry calculation programs.

We also detail the extended QC procedures undertaken to ensure that only the highest quality data were archived and used to generate depth transects. However, because of the tremendous natural variability in this region and the occurrence of strong environmental anomalies during the decade of observations in the data product, we took the approach of flagging data points that may ultimately end up being deemed "bad" measurements (QC flag of 4) as "questionable" (QC flag of 3) to indicate that they deserve further attention by other investigators. Good measurements are marked with a QC flag of 2

3.1 Calculated and adjusted variables

Temperature-independent units are required for carbonate system calculations (Lewis and Wallace, 1988; Gattuso et al., 2022) and are consistent with recommendations of Jiang et al. (2022). Specifically, in order to make carbonate system calculations, phosphate and silicate data were converted to temperature-independent µmol kg^{-1} units for compatibility with the chemical dissociation constants used in *seacarb* or CO_2SYS calculations. Throughout this article, we discuss results using temperature-independent units of µmol kg^{-1}, referred to as "substance content" rather than concentration, which has mg or µmol L^{-1} units. However, the publicly accessible Salish cruise data product includes all parameters in original units as well as those converted to µmol kg^{-1} units for oxygen, phosphate, and silicate concentrations to enable use of this data package with internally consistent units by diverse end users.

3.1.1 Potential density anomaly, or sigma theta (σ_θ), calculations

Potential density (ρ_θ) values, which represent the density of seawater calculated with *in situ* salinity, potential temperature, and pressure referenced to 0 db, were calculated using the 2010 thermodynamic equations of state of seawater (IOC, SCOR, and IAPSO, 2010). Potential density (units of kg m^{-3}) is necessary for converting units from per-liter "concentration" to per-kilogram basis "content" units, as is conventional in chemical oceanography. The potential density anomaly, or sigma theta (σ_θ), is a useful way of comparing the relative densities of different water masses across space, depth, and time, and is provided with the data product but not discussed further in this article as it tracks salinity closely in Puget Sound. σ_θ is calculated simply as:

$$\sigma_\theta = \rho_\theta - 1000\ , \quad (1)$$

https://doi.org/10.5194/essd-2023-239
Preprint. Discussion started: 28 September 2023

and is also expressed in units of kg m^{-3}.

3.1.2 Oxygen unit conversions

All CTD and bottle dissolved oxygen (O_2) data were converted from original units (mg O_2 L^{-1} seawater) to µmol O_2 kg^{-1} seawater using equation 2:

$$O_2\ (in\ \mu mol\ kg^{-1}) = \frac{O_2\ (in\ mg\ L^{-1}) \times 44{,}659.6}{\rho_\theta \times 1.42903}, \quad (2)$$

where ρ_θ is in units of kg m^{-3} as noted above, and 44,569.6 is the reciprocal of the molar volume of O_2 gas, in µmol L^{-1} (from 22,391.6 cm^3 mol^{-1} in García and Gordon, 1992). Conversion factors of 1000 L m^{-3} in the numerator and 1000 mL L^{-1} in the denominator cancel out. For end users preferring O_2 data in units of mL L^{-1}, we also provide the final, recommended O_2 values (Section 3.1.4) in mL L^{-1} in the submitted data product using the conversion:

$$O_2\ (in\ mL\ L^{-1}) = \frac{O_2\ (in\ mg\ L^{-1})}{1.42903\ (in\ mg\ mL^{-1})}, \quad (3)$$

where the conversion factor can be derived from García and Gordon (1992) but a Sea-Bird technical document (Sea-Bird Electronics, 2013) is also often cited.

3.1.3 Density corrections for measurements conducted in laboratory

Nutrient data were also converted to units of µmol kg^{-1} to facilitate subsequent calculations in CO_2SYS or *seacarb*. To do so, the density of seawater under laboratory conditions was calculated following the TEOS-10 thermodynamic equation of seawater (IOC, SCOR, and IAPSO, 2010), using 22 °C for laboratory temperature, 0 db pressure, and *in situ* salinity. After converting density to units of kg L^{-1} (from kg m^{-3}), nutrient concentration measurements in µmol L^{-1} were converted to µmol kg^{-1} by dividing by the calculated laboratory seawater density. Nutrient measurements are submitted in both µmol L^{-1} (original units) and µmol kg^{-1} form to facilitate CO_2SYS and *seacarb* calculations and other end uses.

3.1.4 Adjusting CTD oxygen measurements for offset from bottle oxygen values

We plotted Winkler/bottle O_2 (OXYGEN_UMOL_KG, *y*-axis) against CTD O_2 (CTDOXY_UMOL_KG, *x*-axis) values in µmol kg^{-1} separately for each cruise to determine offset and slope corrections between the two sets of measurements through linear regression. Prior to regression, we inspected all visually apparent outliers in the context of the depth profiles at each station. Oxygen quality flags were not assigned at the time of analysis, although notes were taken on any problems encountered at the time of analysis (e.g., bubbles in titrator or running out of reagent). Samples that had analytical problems noted or that were collected from deep water and had outlying bottle O_2 values were flagged 4, as these values are likely bad for any application, and were not included in the data product. The 4s were identified from samples collected from water depths >25 m with O_2 concentrations that appeared to be from a substantially different depth within a given profile, whether the value appeared to be substantially too low or too high.

Another subset of samples was identified as having mismatches between CTD and bottle O_2 values but where neither value was necessarily bad. These bottle samples were flagged 3 in the submitted data sets, representing questionable data, to denote the mismatch between bottle and CTD measurements. Most of these were collected near the surface and likely just reflect strong

https://doi.org/10.5194/essd-2023-239
Preprint. Discussion started: 28 September 2023

stratification resulting in real differences in the O_2 concentrations measured by the CTD O_2 sensor compared to those in the overlying Niskin bottle sample.

All other samples were presumed to be of acceptable quality and assigned initial QC flags of 2 accordingly. All samples flagged 3 or 4 during inspection were excluded from the regression to avoid introducing leverage into the resulting regression equation, however, many of the samples flagged with 3s may be good for other applications. In total, 178 CTD–bottle O_2 pairs were excluded due to having assigned data quality flags of 3 or 4 out of a total of 6153 pairs (<3%; Table 3).

Table 3. Oxygen correction coefficients and statistics for each cruise.

Cruise dates	Slope (m)	Intercept (b)	r^2	Total number of paired CTD-bottle O_2 measurements	Number of pairs excluded from regression (%)
Feb. 4–8, 2008	1.0239	1.4071	0.9738	344	2 (0.6)
Aug. 11–15, 2008	0.9097	6.8668	0.9875	450	13 (2.9)
Sep. 29–Oct. 2, 2009	0.9974	11.903	0.9843	295	14 (4.7)
Oct. 31–Nov. 3, 2010	1.0417	–0.3001	0.9850	343	7 (2.0)
Oct. 8–14, 2011	1.1123	–2.0014	0.9856	412	5 (1.2)
May 25–26, 2012	1.1077	–2.3810	0.9978	65	2 (3.1)
Apr. 22–23, 2013	1.0675	3.1860	0.9969	69	12 (17.4)
Sep. 22–25, 2013	1.0919	–4.6056	0.9900	89	2 (2.2)
Jul. 14–18, 2014	1.0128	7.6644	0.9803	290	7 (2.4)
Sep. 29–Oct. 3, 2014	1.0182	6.5779	0.9865	289	8 (2.8)
Oct. 22–31, 2014	1.0490	0.1607	0.9909	157	6 (3.8)
Apr. 5–9, 2015	1.0116	8.9541	0.9805	235	5 (2.1)
May 23–24, 2015	1.0379	1.7756	0.9984	99	2 (2.0)
Jul. 7–11, 2015	1.0225	3.4611	0.9893	251	6 (2.4)
Sep. 23–27, 2015	1.0122	4.6005	0.9713	234	10 (4.3)
Nov. 16–19, 2015	1.0508	2.9504	0.9963	106	3 (2.8)
Mar. 17–19, 2016	0.9480	4.0508	0.9894	84	3 (3.6)
Apr. 5–9, 2016	1.0276	3.1942	0.9929	235	5 (2.1)
May 23–24, 2016	1.0222	0.0490	0.9972	16	0 (0.0)
Jul. 7 and 21–25, 2016	1.0220	2.6451	0.9778	235	6 (2.6)
Sep. 21–25, 2016	0.9956	10.0200	0.9790	235	5 (2.1)
Oct. 24–27, 2016	1.1417	–8.2110	0.9832	63	2 (3.2)
Apr. 4–10, 2017	1.0438	6.3659	0.9667	210	3 (1.4)
May 2–5, 2017	1.1137	–3.4906	0.9745	40	3 (7.5)
Jul. 11–15, 2017	0.8066	1.4562	0.9851	238	18 (7.6)
Sep. 11–15, 2017	0.8771	10.848	0.9634	238	4 (1.7)
Oct. 16–18, 2017	1.0534	2.8415	0.9808	32	1 (3.1)
Apr. 7–11, 2018	0.9479	8.4378	0.9648	238	13 (5.5)
May 23–24, 2018	1.0276	6.3819	0.9908	61	4 (6.6)
Jul. 23–27, 2018	0.9714	7.0186	0.9601	233	3 (1.3)
Sep. 11–15, 2018	0.9221	15.815	0.9400	234	3 (1.3)
Oct. 16–19, 2018	1.1072	–7.7106	0.9862	33	1 (3.0)

With the remaining data points, we generated linear regression equations for each cruise (all regression r^2 values were ≥0.94) and used this relationship to adjust the CTD O_2 data for the offset and slope differences from bottle O_2 values. In other words, while we had bottle O_2 data for a subset of all Niskin bottle samples, we generated the bottle-O_2-equivalent value for all CTD O_2 samples by applying the regression relationship to the CTD O_2 data. Coefficients from linear regressions used to adjust CTD O_2 values for all cruises are listed in Table 3 and correspond to this equation:

$$\mathrm{CTDOXY\_UMOL\_KG\_ADJ} = m \times \mathrm{CTDOXY\_UMOL\_KG} + b, \quad (4)$$

https://doi.org/10.5194/essd-2023-239
Preprint. Discussion started: 28 September 2023

where m is the slope and b is the intercept of the regression equation between the Winkler (OXYGEN_UMOL_KG) and CTDOXY_UMOL_KG values (Table 3). The variable CTDOXY_UMOL_KG_ADJ in the submitted data files are the CTD oxygen values adjusted in this manner. Regression slope values ranged from 0.81 to 1.14, with intercepts from 0.05 to 15.8 µmol kg^{-1}.

Finally, we created a hybrid oxygen column consisting of all Winkler O_2 data with "acceptable" quality, with CTDOXY_UMOL_KG_ADJ filling missing values; this parameter is called RECOMMENDED_OXYGEN_UMOL_KG. The recommended O_2 data column is also provided in both mg L^{-1} and mL L^{-1} units to facilitate adoption by various end user communities. The conversion of recommended O_2 values from µmol kg^{-1} to mg L^{-1} and mL L^{-1} was done by rearranging equations (2) and (3).

3.2 Extended quality control

Extended quality control consisted of preparation of property-property plots after any samples flagged as 4s (=bad value) were eliminated and interpolated pressure vs. along-transect-distance plots (or "depth-transect plots"). Property-property plots were made of parameters that normally show strong correlations with each other (Figures 2–3). Following the recommendations of Jiang et al. (2021) for CODAP-NA data sets, we prepared the following plots: 1) CTDSAL against CTDTMP, 2) TA against CTDSAL, 3) TA against silicate, 4) TA against DIC, 5) DIC against CTDOXY, 6) phosphate against nitrate, 7) nitrate against silicate, and 8) all nutrients (silicate, phosphate, nitrate, nitrite, and ammonium) against CTDOXY. Outliers were again compared to nearby depth and station samples within their cruise and flagged as 3 or 4 as appropriate. All data in the Salish cruise data product with QC flags of 3 were excluded from statistical summaries. However, their distributions are retained in gray in property-property plots to provide end users more information about how likely the data are to be useful for their applications (Figures 2–3).

Interpolated depth transects prepared in Golden Software's *Surfer* program visually depict cross-sections of oceanographic parameters along transects from the coast into Puget Sound for S2S cruises (Figure 4) and from Admiralty Reach along transects toward the terminus of each basin for Puget Sound cruises (Figures 5–9). Outliers identified on depth-transect plots typically manifest as a "bullseye" pattern corresponding to a single sample. Bullseye points were evaluated and reassigned a quality flag of 4 if it was ascertained that the value was likely bad (e.g., due to a Niskin bottle firing at the wrong depth or a sample bottle having been improperly preserved or sealed between collection and analysis) rather than a correctable data entry error. Outliers that changed distributions of oceanographic parameters in the depth transects were subsequently excluded from the cross-sections.

Offsets due to strong stratification in surface waters may yield apparent outliers in such property-property plots comparing CTD sensor data with Niskin bottle analysis data or bottle samples collected sequentially (e.g., Winkler O_2 vs. DIC, TA, or nutrients). In the property-property plots described above, salinity and temperature are based on sensor measurements associated with the CTD package, oxygen data were derived from both CTD sensor and bottle measurements, and DIC, TA, and nutrient measurements were conducted on bottle samples collected some distance above the CTD sensors. While both sensor and discrete bottle sample data in such comparisons may represent accurate measurements, particularly in stratified surface waters, we applied quality flags of 3 (questionable) to the Niskin data of disagreeing sample pairs to reflect the fact that the CTD-bottle sample pairs may not be suitable for all end uses (e.g., as described in Section 3.1.4). For instance, using paired sensor and bottle data from strongly stratified surface waters could yield unreliable empirical relationships (*cf.* Alin et al., 2012; Fassbender et al., 2017).

https://doi.org/10.5194/essd-2023-239
Preprint. Discussion started: 28 September 2023

4 Results

4.1 Sampling coverage and extended quality control of the 2008–2018 Salish cruise data product

To differentiate the distributions of physical and biogeochemical parameters across seasons in the Salish cruise data product, we defined the four seasons as fall (October–November), winter (January–March), early upwelling season (April–May), and late upwelling season (July–September) (months not listed were not sampled on cruises included in the 2008–2018 Salish cruise data product). Collectively, the 2008–2018 Salish cruise data product includes oceanographic observations from 715 profiles, with 144 profiles collected during the early upwelling season (April–June), 338 during the late upwelling season (July–September), and 181 during fall (October–November) (Table 4). As in many regions, the fewest cruise observations were collected during winter conditions (52 profiles for January–March) (*cf.* Benway et al., 2016; Jiang et al., 2021). Late upwelling season profiles occurred during more years across the cruise time-series than during early upwelling season or fall months, and profiles collected during winter months only occurred during 1–2 years in any basin. Across the region, the fewest profiles in this data product were collected in coastal waters. The largest number of profiles were collected in Hood Canal, which received the most sampling effort due to the need to understand variability in oxygen and acidification conditions at this location known to experience recurring seasonal hypoxia.

Table 4. Numbers of profiles and years sampled in each basin by season. Months sampled in each season are indicated in each column header.

Region	Early upwelling season (Apr.–May)		Late upwelling season (Jul.–Sep.)		Fall (Oct.–Nov.)		Winter (Jan.–Mar.)		Total Profiles
	Profiles	Years	Profiles	Years	Profiles	Years	Profiles	Years	
Coast	16	7	9	3	13	6	4	2	42
Strait of Juan de Fuca	25	6	37	8	37	7	9	2	108
Admiralty Inlet	15	5	44	8	16	4	6	2	81
Main Basin	23	4	62	8	35	8	12	2	132
South Sound	12	4	32	6	18	4	4	1	66
Whidbey Basin	16	4	49	7	12	4	5	1	82
Hood Canal	37	4	105	7	50	4	12	1	204

Sensor measurements of temperature, salinity, and oxygen are the most numerous observations across the Salish cruise profiles (n = 7525, 7525, and 7491, respectively), and very few of measurements reflected "questionable" values (i.e., QC flags of 3, with 3, 29, and 9 total observations, respectively) (Table 5). A few CTD profiles appeared to have higher than expected salinity values throughout the water column and received QC flags of 3, while individual measurements near the surface flagged 3 (questionable) may simply reflect strong near-surface stratification and be valid measurements.

Table 5. Numbers of high-quality measurements (QC flags of 2 or 6) in the Salish cruise data product for temperature (T, ITS-90), salinity (S, PSS-78), adjusted CTD oxygen (O_2), discrete ("Winkler") O_2, dissolved inorganic carbon (DIC), total alkalinity (TA), and nutrients by basin. Numbers of measurements of "questionable" quality (QC flags of 3) that are included in the data product and may be useful for some applications are indicated in parentheses.

Region	T	S	CTD O_2	Winkler O_2	DIC	TA	Nutrients
Coast	534 (0)	534 (0)	504 (1)	407 (27)	330 (8)	326 (11)	438 (2)
Strait of Juan de Fuca	1021 (0)	1019 (2)	1019 (2)	849 (8)	700 (11)	717 (8)	833 (25)
Admiralty Inlet	755	755	755	570	449	461	576

https://doi.org/10.5194/essd-2023-239
Preprint. Discussion started: 28 September 2023

	(1)	(1)	(1)	(5)	(5)	(2)	(7)
Main Basin	1579	1569	1574	1282	808	905	1335
	(0)	(10)	(0)	(40)	(21)	(17)	(11)
South Sound	711	703	710	520	364	385	543
	(0)	(8)	(1)	(13)	(8)	(14)	(7)
Whidbey Basin	814	813	815	679	419	442	690
	(2)	(3)	(1)	(19)	(9)	(16)	(9)
Hood Canal	2108	2103	2105	1593	1296	1352	1679
	(0)	(5)	(3)	(58)	(34)	(39)	(14)

Discrete measurements of oxygen via Winkler titration were conducted on 6070 samples. Of these, 170 Winkler O_2 values were assigned QC flags indicating "questionable" quality and eight were flagged 4, indicating "bad" quality that were not submitted (reflected as QC flags of 5, meaning "not reported" in the data product) (Table 5, Figure 2A). Of the questionable quality samples, 74% were shallower than 23 db, with 65% in the top 12 db of the water column. Most Winkler O_2 data with 3 flags also likely reflect strong near-surface stratification rather than questionable measurements (as explained in Section 3.2 and tallied in Table 3). Jiang et al. (2021) also observed near-surface sample mismatches between discrete and CTD O_2 measurements in coastal data sets and concluded that these samples likely reflected true differences between conditions measured by CTD sensors and bottle oxygen samples measurements due to slight differences in depth and strong near-surface stratification.

Dissolved inorganic carbon and total alkalinity measurements (*n*= 4462 and 4695, respectively) received the most thorough initial QA/QC attention (following SOPs in Dickson et al., 2007), having been assigned QC flags immediately after laboratory analyses were conducted based on instrument diagnostics (with 90 and 101 QC=3 flags assigned to DIC and TA at this stage) or routine plots generated in the process of finalizing the data (Table 5). Additional "questionable" QC flags were assigned during extended QC to six samples each for DIC and TA, with some overlap, based on property-property plots against salinity.

Nutrient analyses were conducted on 6169 samples (Table 5). These cruises did not have nutrient sensors, and nutrient data were not QC flagged by the laboratory providing the data. We assigned 150 nutrient observations QC flags of 3, using the property-property plots recommended by Jiang et al. (2021) to identify outliers (Figure 2B–H). While a number of these plots showed significant scatter, we took a conservative approach to flagging outliers, assigning no flags of 4, with the recognition that many of these outliers may reflect either freshwater influence or redox or biological conditions caused by environmental anomalies such as the marine heatwave conditions of 2014–2016 (*cf.* Alin et al., 2023b). Thus, we suggest that other apparent nutrient outliers deserve further scrutiny before concluding they are necessarily "questionable" or "bad" measurements. We flagged all nutrients as "questionable" when only one parameter may have been an outlier, with the rationale that the full suite of nutrient measurements for that sample may warrant further attention.

In total, the Salish cruise data product consists of 3963 observations for which the full suite of inorganic carbon, oxygen, nutrient, and CTD measurements are available, with all parameters having QC flags of 2 or 6 after extended QC, indicating "acceptable" quality measurements. These highest quality, co-located measurements are the core of the Salish cruise data product most suitable for assessing multiple stressor conditions such as co-occurring marine heatwaves, hypoxia, and ocean acidification. This subset of the data can be used without further modification for CO_2SYS or *seacarb* calculations and is provided as a separate CSV data product for end users wishing to perform CO_2 system calculations without having to further consider data that may be "questionable." For end users who prefer to either apply average nutrient concentrations or zero values for nutrient measurements that are missing or flagged for calculating the full CO_2 system, there are an additional 305 sets of observations of DIC, TA, temperature, and salinity (with 150 of these being "questionable" nutrient values that may be found to be of acceptable quality

https://doi.org/10.5194/essd-2023-239
Preprint. Discussion started: 28 September 2023

after further analysis). Finally, for end users with the capacity to conduct additional QC, especially on nutrient measurements, and/or interpolate any of the missing values for a desired analysis, the full data set of 7525 observations, including measurements with QC flags of 3, is also available. All three subsets of the Salish cruise data product are available on the NOAA National Centers for Environmental Information web site as described in Section 7.

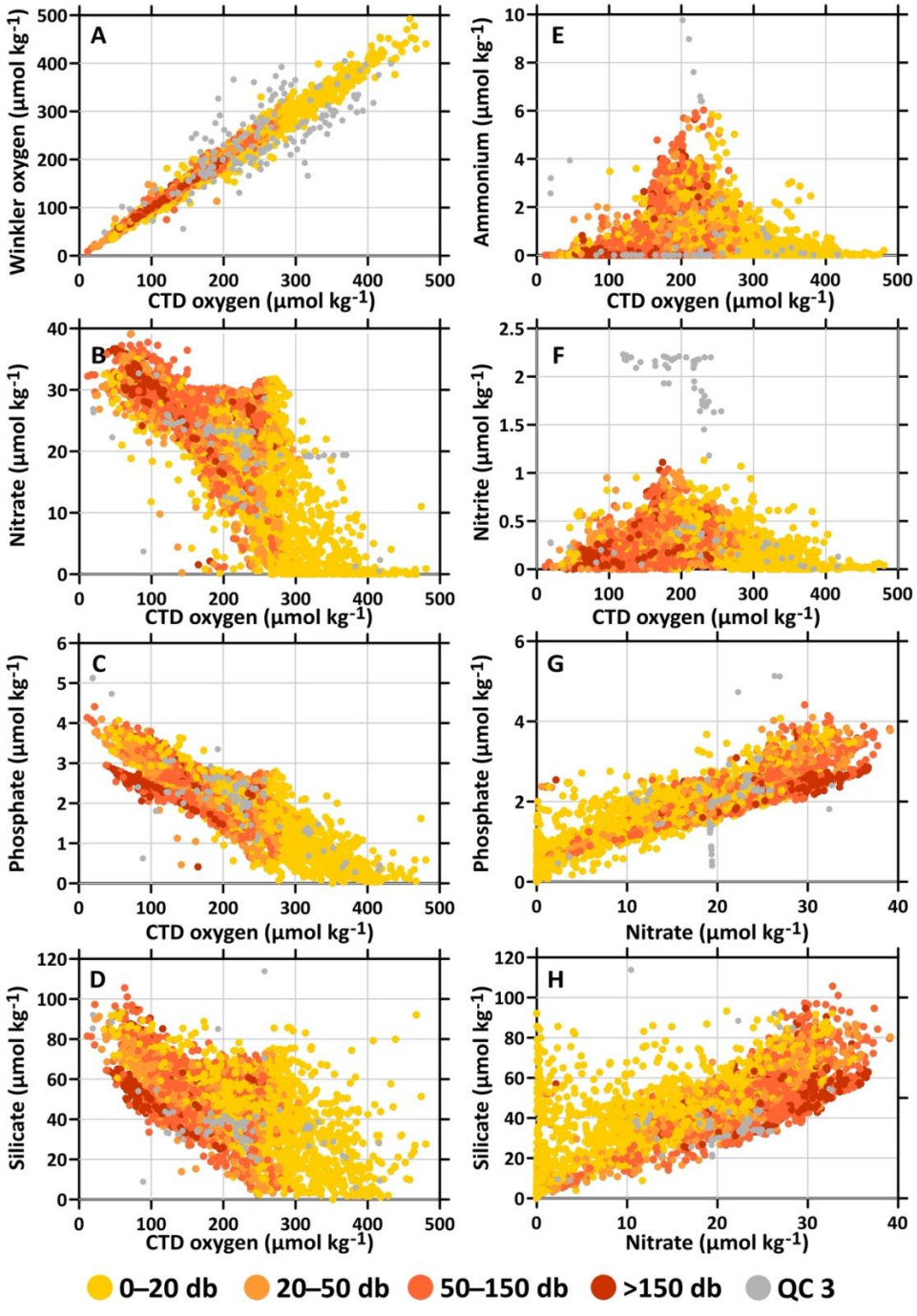

https://doi.org/10.5194/essd-2023-239
Preprint. Discussion started: 28 September 2023

Figure 2: Property-property plots of oceanographic parameters used to detect data with potential sampling or analytical problems. A) CTD oxygen (CTDOXY_UMOL_KG_ADJ) vs. Winkler oxygen (OXYGEN_UMOL_KG) content; B) CTD oxygen vs. nitrate (NITRATE_UMOL_KG) content; C) CTD oxygen vs. nitrite (NITRITE_UMOL_KG) content; D) CTD oxygen vs. ammonium (AMMONIUM_UMOL_KG) content; E) silicate (SILICATE_UMOL_KG) vs. total alkalinity (TA_UMOL_KG) content; F) dissolved inorganic carbon (DIC_UMOL_KG) vs. nitrate content; G) phosphate (PHOSPHATE_UMOL_KG) vs. nitrate content; and H) silicate for all observations with QC flags of 2 (acceptable) for both parameters, and measurements with QC flags of 3 (questionable) for either parameter are gray.

4.2 Range and spatial distribution of oceanographic conditions across the Salish cruise study region

Oceanographic parameters spanning the region from Washington's coastal waters to the interior parts of each sub-basin of the southern Salish Sea occupied broad ranges of values. Summary statistics are provided in Table 6, though it should be noted that observations in this discrete sample data product are biased toward shallower depths; 40% of observations were collected ≥20 db and 63% ≥50 db, compared to 31% from >50–150 db and <7% >150 db (see symbol color in Figure 2). Parameters were often distributed similarly across boundary waters stations (coast, Strait of Juan de Fuca), Puget Sound stations from more well-mixed basins (Admiralty Reach, Main Basin, South Sound), and more stratified Puget Sound stations (Whidbey Basin, Hood Canal), but summary statistics are provided in Table 6 by individual basin. Temperatures across the region and water column spanned 6.0–21.8 °C, with the lowest measurements in deep coastal waters and the highest in Hood Canal surface waters (Figures 2 and 4–5). Salinity spanned 15.6–34.0, with all but two of the acceptable salinity values <25 occurring in the stratified WB and HC basins, and the highest salinity in deep coastal waters (Figures 4 and 6). Adjusted CTD O_2 values had their lowest and highest values in Hood Canal's deep and surface waters, respectively, spanning 12–481 µmol kg^{-1} overall (Figures 4 and 9). Both DIC and TA had their minimum observations in surface HC waters (1074 and 1274 µmol kg^{-1}, respectively), while their maxima occurred in deep SJdF waters (2362 and 2296 µmol kg^{-1}), likely reflecting canyon-enhanced upwelling via the Juan de Fuca Canyon (Figures 4 and 7–8). Minimum phosphate measurements approached zero in all areas, with maxima of 2.6–3.0 µmol kg^{-1} in all basins except in WB and HC, where maxima reached 3.8–4.4 µmol kg^{-1} (Table 6, Figures S1–S2). Silicate content had wide ranges across the region, with the lowest minimum values of 0.0–1.5 µmol kg^{-1} in boundary waters and the highest maxima of 85.4–113.8 µmol kg^{-1} in WB and HC (Figures S1–S3). Nitrate content had similar ranges across the region, with minima of 0.0–1.1 µmol kg^{-1} and maxima spanning 31.1–39.1 µmol kg^{-1} (Figures S1–S4).

Table 6. Summary statistics (minimum–maximum (median ± standard deviation)) for temperature (T, ITS-90), salinity (S, PSS-78), adjusted CTD oxygen (O_2), dissolved inorganic carbon (DIC), total alkalinity (TA), phosphate, silicate, and nitrate by basin.

Region	T (° C)	S	O_2 (µmol kg^{-1})	DIC (µmol kg^{-1})	TA (µmol kg^{-1})	Phosphate (µmol kg^{-1})	Silicate (µmol kg^{-1})	Nitrate (µmol kg^{-1})
Coast	6.0–15.6 (9.3±2.5)	28.2–34.0 (32.5±1.0)	47–417 (215±89)	1838–2344 (2103±122)	1984–2284 (2196±51)	0.0–2.9 (1.5±0.8)	1.5–65.0 (26.3±19.2)	0.0–36.7 (15.7±12.3)
Strait of Juan de Fuca	6.6–15.2 (9.5±1.4)	28.6–33.9 (31.4±1.3)	38–429 (182±56)	1807–2362 (2084±88)	2013–2296 (2146±58)	0.0–3.0 (2.2±0.4)	0.0–64.5 (44.7±9.2)	0.0–36.2 (24.2±6.0)
Admiralty Inlet	7.3–14.6 (10.8±1.5)	27.4–32.8 (30.6±0.8)	101–349 (198±39)	1713–2195 (2042±59)	1939–2218 (2107±42)	0.3–2.6 (2.1±0.3)	5.9–68.9 (42.6±7.7)	1.1–31.1 (21.2±4.4)
Main Basin	7.5–16.5 (11.6±1.9)	24.0–31.2 (29.9±0.8)	148–419 (209±47)	1637–2148 (1996±66)	1799–2150 (2071±43)	0.0–2.7 (2.1±0.4)	2.1–67.8 (45.0±10.1)	0.0–31.8 (21.8±5.8)
South Sound	6.8–16.8 (13.0±2.4)	27.1–30.5 (29.3±0.7)	136–432 (227±44)	1692–2119 (1956±58)	1928–2115 (2050±39)	0.4–2.7 (2.1±0.4)	9.3–74.8 (46.0±11.0)	0.8–31.5 (16.7±6.5)
Whidbey Basin	6.5–18.6 (11.3±2.1)	19.8–31.1 (29.3±2.1)	88–458 (203±76)	1316–2125 (1990±163)	1452–2130 (2035±112)	0.1–3.8 (2.3±0.7)	4.7–85.4 (48.3±15.9)	0.0–34.9 (23.0±8.8)
Hood Canal	6.9–21.8 (10.9±2.2)	15.6–31.4 (29.8±1.5)	12–481 (168±83)	1074–2217 (2040±129)	1274–2143 (2067±72)	0.1–4.4 (2.5±0.8)	2.1–113.8 (55.7±16.7)	0.0–39.1 (24.2±9.5)

https://doi.org/10.5194/essd-2023-239
Preprint. Discussion started: 28 September 2023

Across the decade-long cruise time-series, separation in the seasonal and spatial distributions of the core parameters of temperature, salinity, TA, DIC, and oxygen—which are the most critical for assessing variations in marine heat, hypoxia, and acidification—can be visualized to more fully delineate the distinct water mass characteristics across the region using depth transects (Figures 3–9). Late upwelling season and fall temperatures were higher than those in winter and the early upwelling season, with the broadest salinity ranges observed during the upwelling season (Figures 3A and 4). Together, the T-S distributions were widest, with the greatest scatter in both T and S values in the stratified basins, with more concentrated T and S values in the middle of the full range in the well-mixed PS regions, and most of the highest S, lowest T values clustering in boundary waters (Figures 3B, 4–5).

For the most part, the relationship between salinity and alkalinity was linear and overlapped across seasons and basins (Figures 3C and 6–7), but fall and winter mostly had higher values of both S and TA, while upwelling season TA and S occupied the full range of values seen in both parameters, with wider scatter at low S and TA values reflecting the input of rivers with a wide range of TA end-member values (e.g., Voss et al., 2014; Banas et al., 2015; Bianucci et al., 2018; Moore-Maley et al., 2018). Spatially, boundary waters more typically had high TA and S values, well-mixed PS basins had moderate values, and stratified PS basins had the lowest TA and S values (Figures 3D and 6–7).

Overall, DIC and alkalinity had a less linear relationship across the region (Figure 3E–F) than salinity and alkalinity. The highest DIC and TA values were observed across seasons in boundary waters and appeared to have a shallower and more linear slope than Puget Sound basins. Within PS, the more stratified basins had the broadest, least linear relationship, with a distinct flattening of TA values at the highest DIC values in stratified basins, which occurs during the late upwelling season into fall, when DIC accumulations are relatively high there (Feely et al. 2010, Blue Ribbon report, Alin 2023). Depth transects show that the magnitude of seasonal changes in TA are not as large as the seasonal changes in DIC in deep waters of the stratified basins, particularly in HC (Figures 7–8).

Seasonal consumption of oxygen and enrichment of DIC by respiration drive the development of hypoxic and acidified conditions in the region (Feely et al., 2010, 2023). The relationship between DIC and O_2 is linear over the high DIC, low O_2 end of the distribution, across seasons and basins, reflecting the stoichiometric linkage between CO_2 and O_2 via respiration processes (Figure 3D and 3H). The greater scatter among higher O_2, lower DIC observations, which occur in surface waters, reflects in part that O_2 and CO_2 have vastly different gas exchange rates with the atmosphere (Wanninkhof, 2014), which reduces the linearity of the relationship between CO_2 and O_2 typically seen in subsurface waters. Higher DIC and lower O_2 values tend to occur during the late upwelling season through winter across the region (Figures 3G and 8–9). The distribution of DIC values relative to O_2 content also differs between the coast and Puget Sound, with boundary water stations having higher DIC for the same O_2 levels compared to Puget Sound basins, with stratified basins having the lowest DIC relative to O_2 levels (Figure 3H). The most hypoxic and acidified conditions observed in the region covered by this data compilation typically occur in the southern end of HC (Feely et al., 2010; Alin et al., 2023b). In addition to the important role respiration plays in creating the hypoxic, acidified conditions seen in southern HC, mixing and river input contribute to the separation of the DIC vs. O_2 data distribution on the coast vs. in Puget Sound. Strong mixing of deep upwelled marine water entering Puget Sound through Admiralty Reach with river-influenced surface waters both equilibrates O_2 from deep waters with the atmosphere more than it equilibrates CO_2 (*sensu* Ianson et al., 2016) and mixes surface water with relatively high O_2 and low DIC and TA content from regional rivers to depth. Further mixing occurs as denser incoming marine waters transit another glacial sill going from Admiralty Reach into Hood Canal. Together, these processes contribute to lower PS DIC and TA and higher O_2 in deep PS waters, and particularly in HC, than in upwelled coastal waters. The

https://doi.org/10.5194/essd-2023-239
Preprint. Discussion started: 28 September 2023

highest O_2 and lowest DIC conditions occur in surface waters predominantly during the upwelling season, again with lower DIC for the same O_2 level in PS basins than along the coast. Mixing during winter provides nutrient supply to the surface water during spring and summer; this coinciding with longer daylengths fuels production that is subsequently respired at depth (Figures S1–S4 show distributions of the major nutrients phosphate, silicate, and nitrate through the study region and seasons). The hypoxic, acidified waters from deep HC are often pushed up to mid-depth during fall if the seasonal oceanic intrusion is denser (e.g., HC panels from Oct. 2010 and Sept 2018 in Figures 8–9).

https://doi.org/10.5194/essd-2023-239
Preprint. Discussion started: 28 September 2023

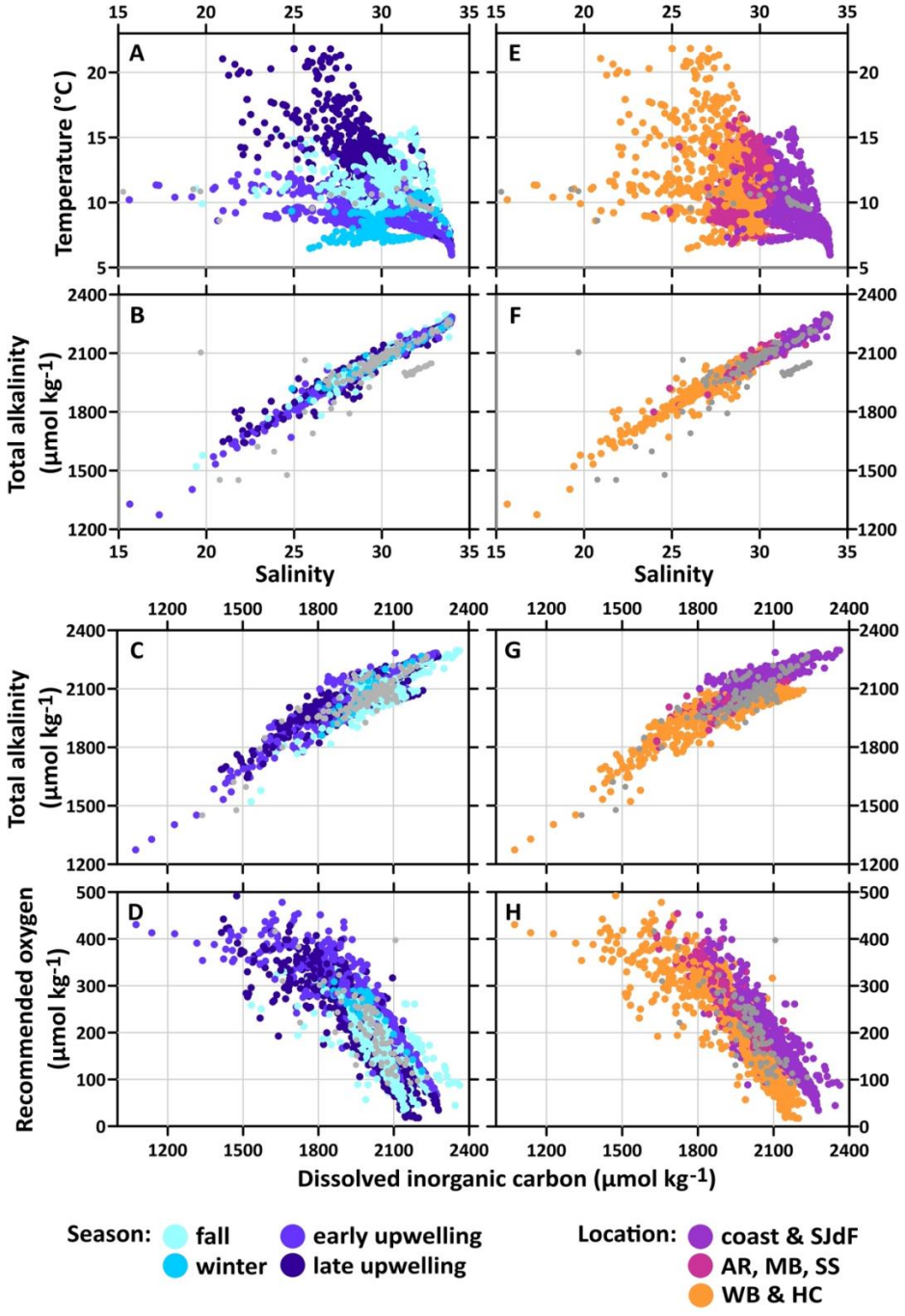

Figure 3: Property-property plots of oceanographic parameters used to delineate spatial and seasonal variability: salinity (CTDSAL_PSS78) vs. temperature (CTDTMP_DEG_C_ITS90) by season (A) and location (E), salinity vs. total alkalinity (TA_UMOL_KG) by season (B) and location (F), dissolved inorganic carbon (DIC_UMOL_KG) vs. total alkalinity by season (C) and location (G), and CTD oxygen (CTDOXY_UMOL_KG_ADJ) vs. dissolved inorganic carbon by season (D) and location (H). Seasons are fall (October–November), winter (January–March), early upwelling (April–May), and late upwelling (July–September). Stations are colored separately for boundary waters (coast and Strait of Juan de Fuca), well-mixed Puget Sound (Admiralty Reach, Main Basin, and South Sound), and stratified Puget Sound basins (Whidbey Basin, Hood Canal). All observations with a QC flag of 3 (questionable) for either parameter appear in gray.

https://doi.org/10.5194/essd-2023-239
Preprint. Discussion started: 28 September 2023

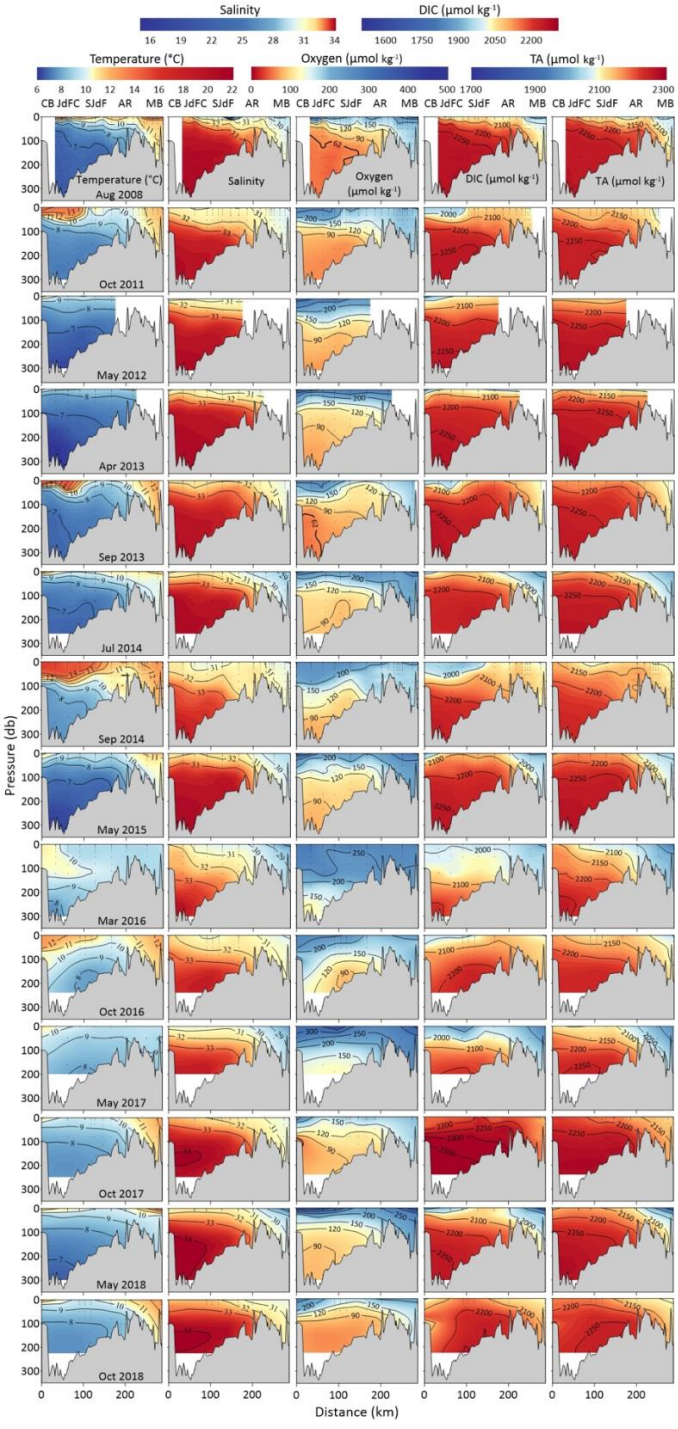

Figure 4: Depth transect plots from Sound-to-Sea cruises for CTD temperature, salinity, adjusted CTD oxygen, dissolved inorganic carbon, and total alkalinity in respective columns. The month and year when each cruise began is indicated in left panel of each row. 555 **Each panel shows ocean conditions starting at the Ćháʔba· mooring (CB), traveling through the Juan de Fuca Canyon (JdFC) and the Strait of Juan de Fuca (SJdF), over the glacial sills in Admiralty Reach (AR), and into the Main Basin (MB) of Puget Sound as the distance along transect increases (see map in Figure 1). Color scales are the same for each parameter across Figure 4 and the comparable Puget Sound figures (Figures 5–9).**

https://doi.org/10.5194/essd-2023-239
Preprint. Discussion started: 28 September 2023

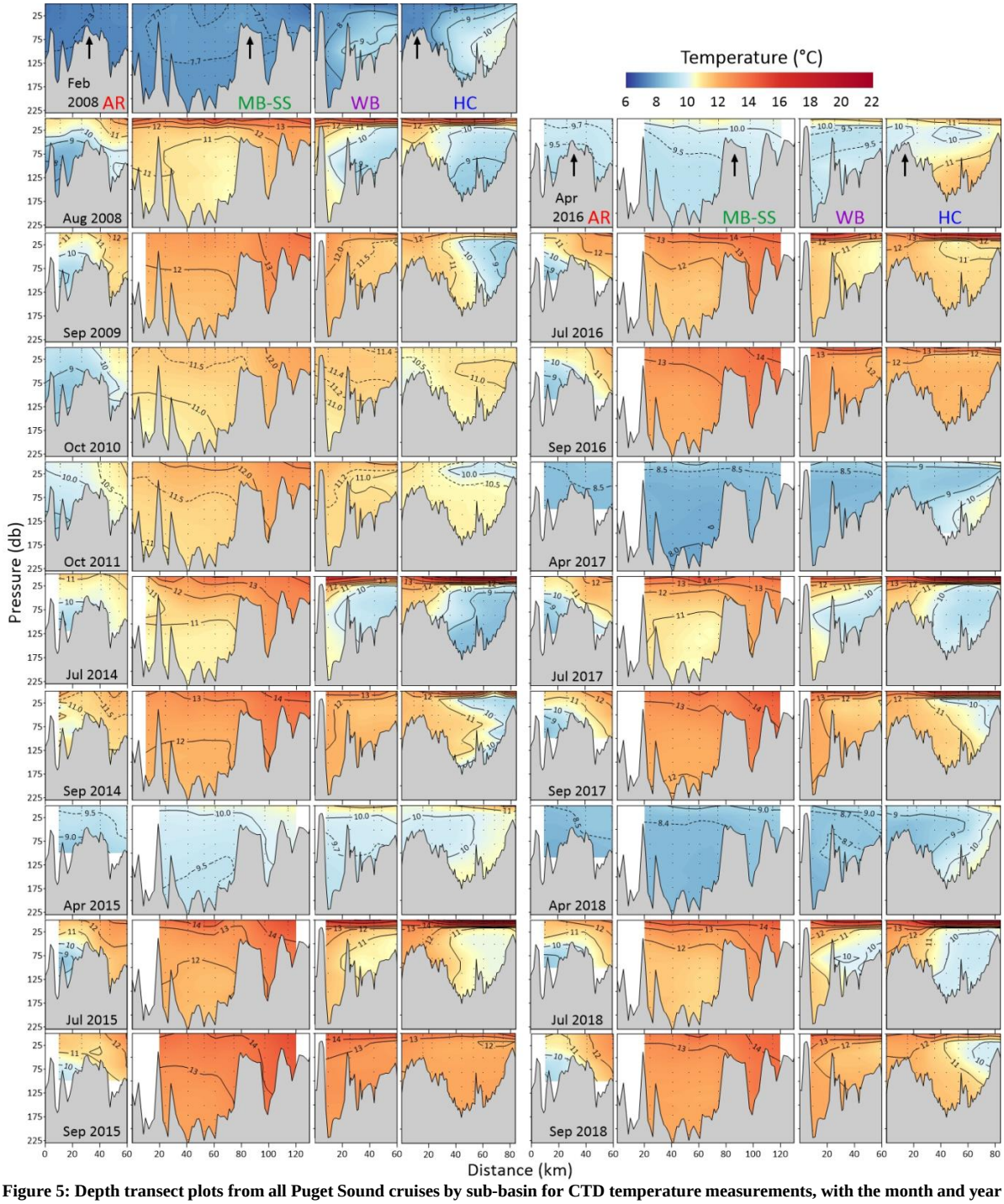

Figure 5: Depth transect plots from all Puget Sound cruises by sub-basin for CTD temperature measurements, with the month and year when each cruise began indicated in the left panel of each row, noting that there are two columns consisting of four panels each to encompass all cruises. From left to right, panels within each column correspond to Admiralty Reach (AR), Main Basin–South Sound (MB–SS), Whidbey Basin (WB), and Hood Canal (HC). Colours of abbreviations correspond to station colours in Figure 1. Admiralty Reach panels show the bathymetric profile and ocean conditions from the Strait of Juan de Fuca (SJdF) on the left going through Admiralty Reach toward Puget Sound on the right. The other three panels start at the nearest point on their respective transects inside Puget Sound from Admiralty Reach and progress to the distal end of the transects shown in the Figure 1 inset map as distance along transect increases.

https://doi.org/10.5194/essd-2023-239
Preprint. Discussion started: 28 September 2023

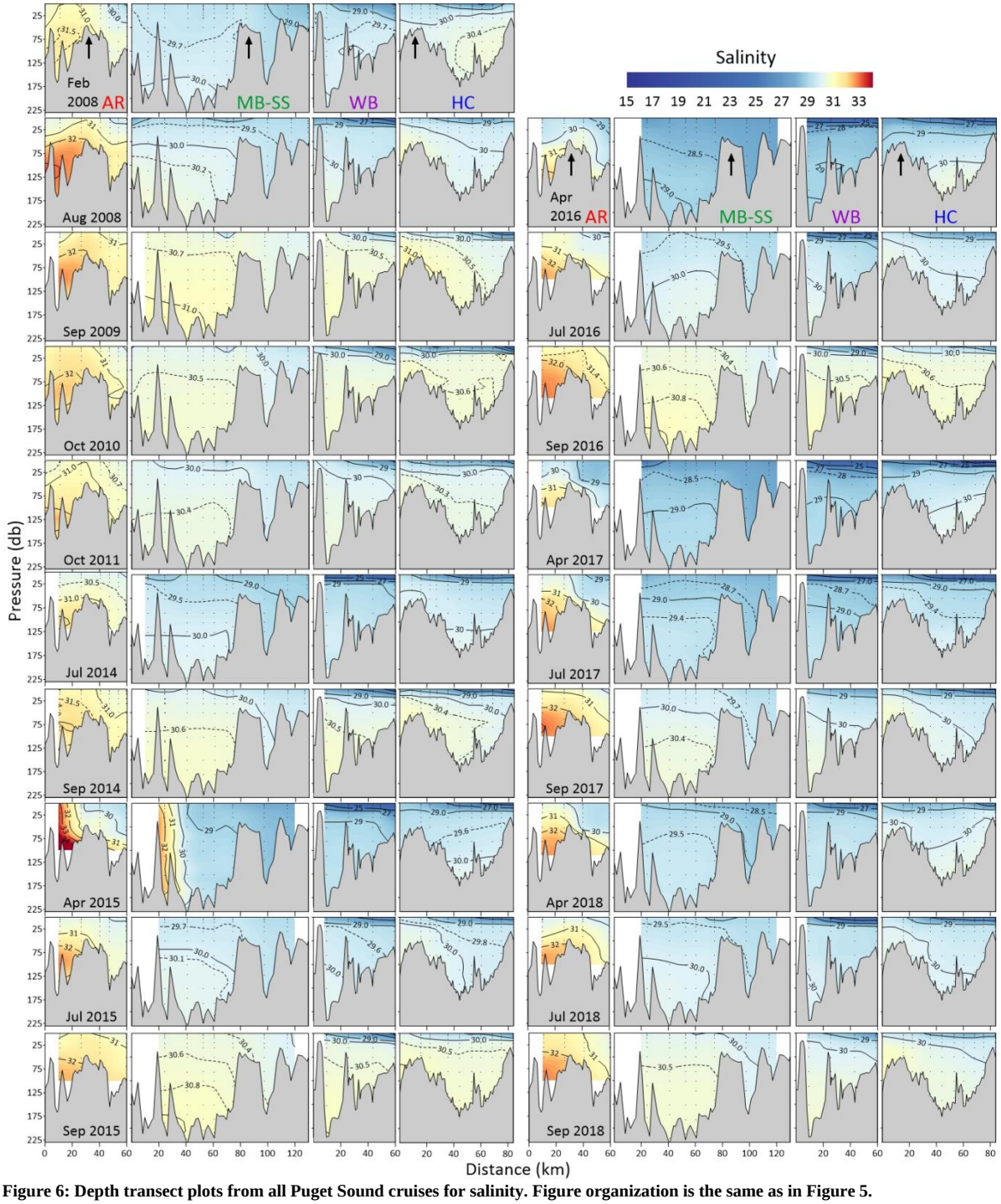

570 **Figure 6: Depth transect plots from all Puget Sound cruises for salinity. Figure organization is the same as in Figure 5.**

https://doi.org/10.5194/essd-2023-239
Preprint. Discussion started: 28 September 2023

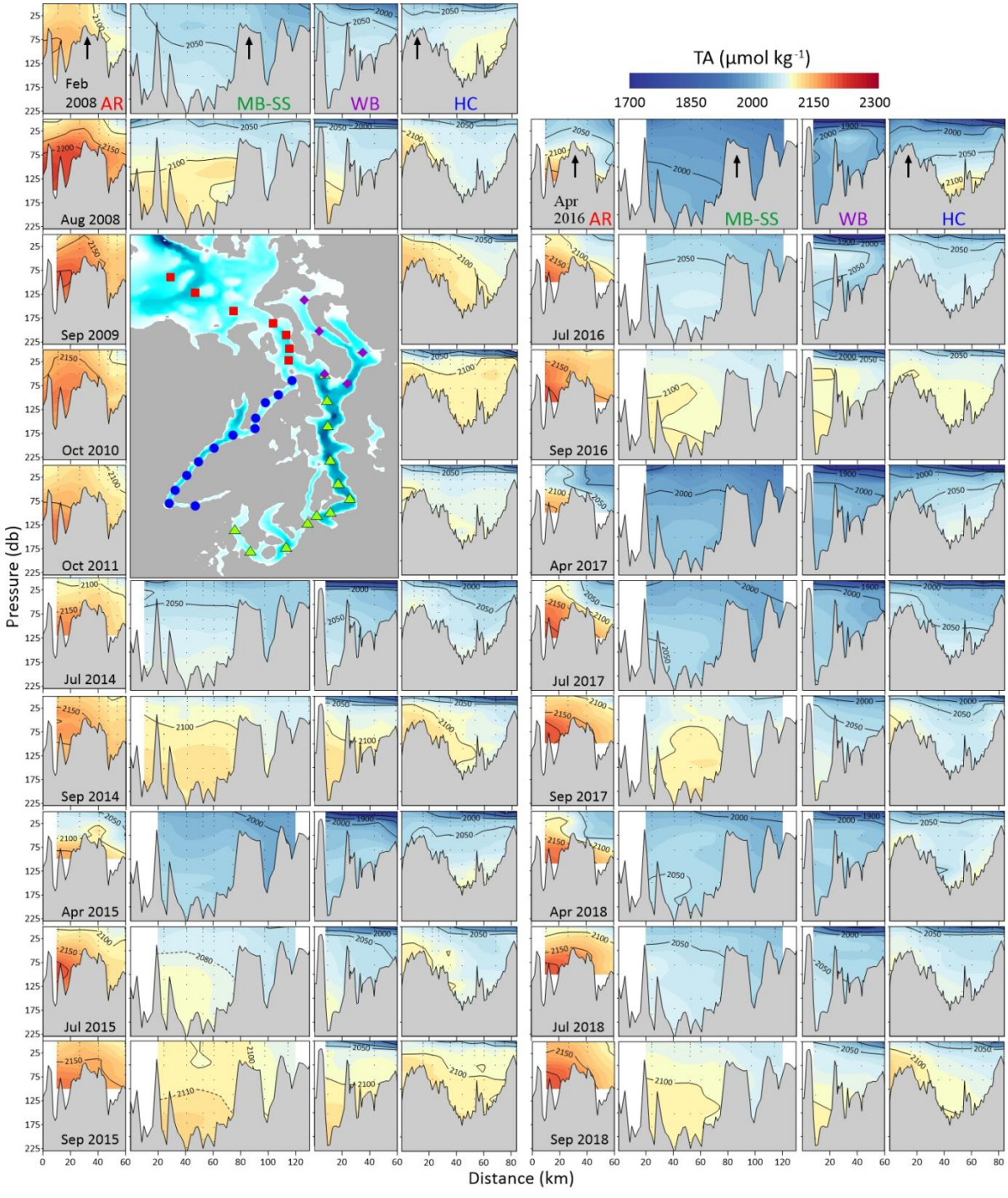

Figure 7: Depth transect plots from all Puget Sound cruises for total alkalinity content (TA, µmol kg^{-1}). Figure organization is the same as in Figure 5. The inset map shows sampling stations and is shown in place of data profiles for cruises that were not sampled for inorganic carbon parameters.

https://doi.org/10.5194/essd-2023-239
Preprint. Discussion started: 28 September 2023

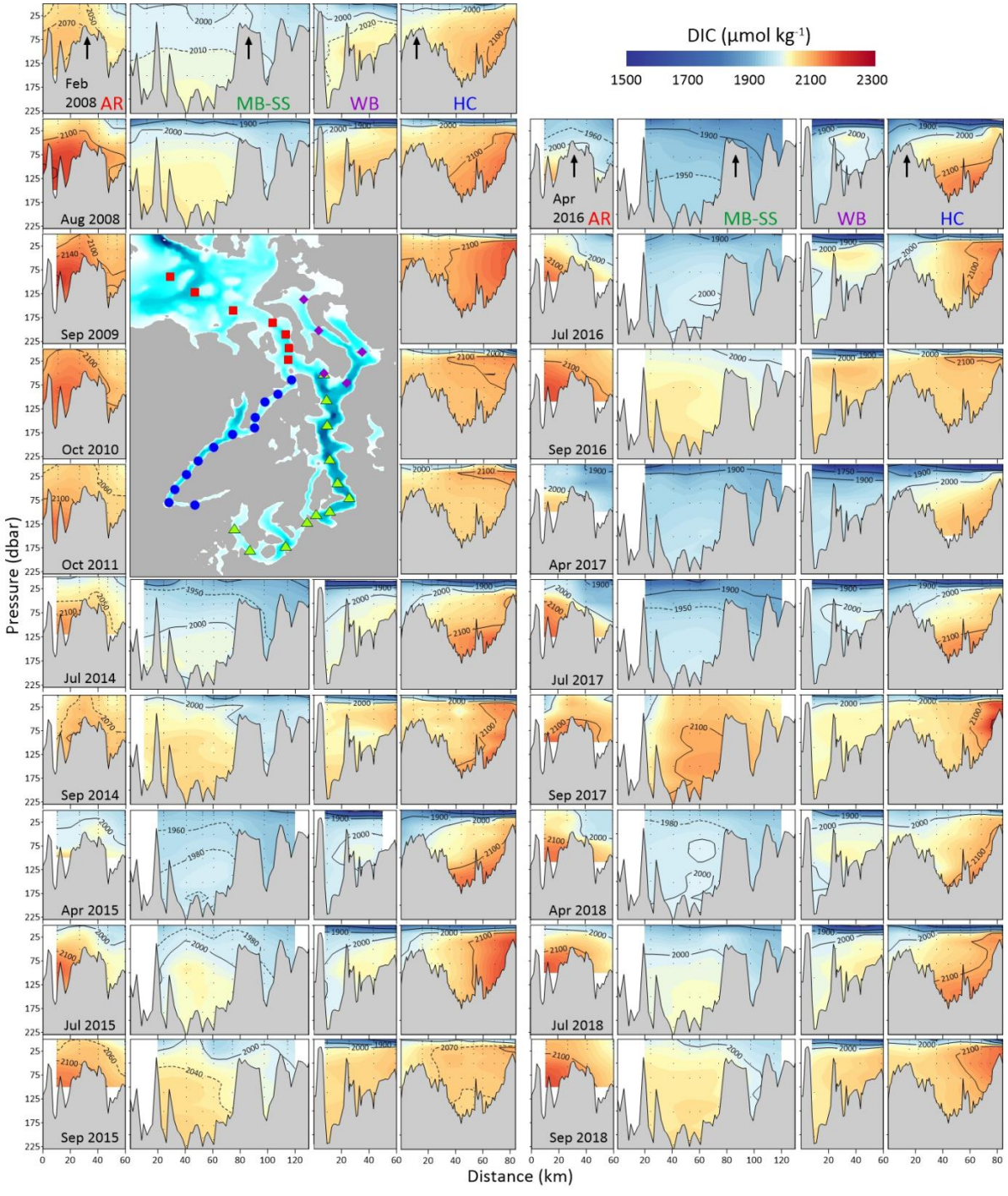

575

Figure 8: Depth transect plots from all Puget Sound cruises for dissolved inorganic carbon content (DIC, µmol kg^{-1}). Figure organization is the same as in Figure 5. The inset map shows sampling stations and is shown in place of data profiles for cruises that were not sampled for inorganic carbon parameters.

https://doi.org/10.5194/essd-2023-239
Preprint. Discussion started: 28 September 2023

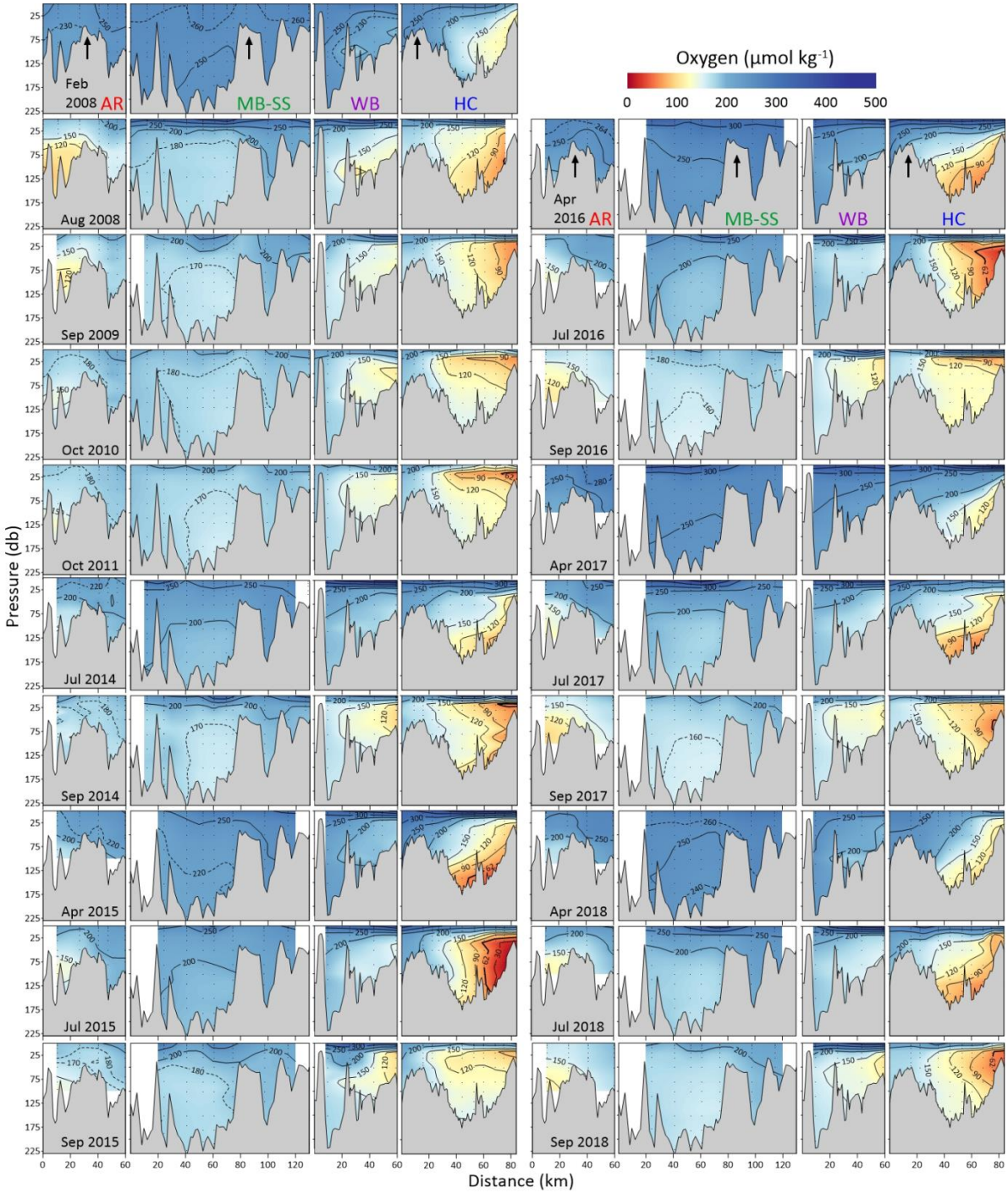

580 **Figure 9: Depth transect plots from all Puget Sound cruises for adjusted CTD oxygen content (O_2, µmol kg^{-1}). Figure organization is the same as in Figure 5.**

https://doi.org/10.5194/essd-2023-239
Preprint. Discussion started: 28 September 2023

5 Applications and limitations of the Salish cruise data product

5.1 Using the Salish cruise time-series to understand ecological impacts of climate and ocean change

5.1.1 Past applications

A number of studies have already used Salish cruise data from this data product to describe variability in ocean conditions and provide context for understanding the physiological condition of and response to ocean acidification conditions for regionally important species, under both current and projected scenarios. For example, cruises included in this data product through 2014 were included in a large data compilation used to create seasonal climatologies for salinity, temperature, DIC, TA, and the calculated CO_2 system parameters CO_2 fugacity (fCO_2), pH (on the total scale), aragonite saturation state (Ω_{arag}), and Revelle factor (a buffering capacity metric), allowing end users to assess the range of average surface conditions expected in Washington's marine ecosystems (Fassbender et al., 2018). The same data compilation underpinned the development of an empirical TA-S relationship in Washington's marine surface waters (0–25 m) that allows users to estimate TA data using salinity as a proxy (Fassbender et al., 2017), providing end users a second surface carbon parameter for use in calculating the full CO_2 system and assessing acidification levels in ecosystems or stations with only a single carbon data stream. This approach could be especially useful for understanding conditions in nearshore ecosystems, where full constraint of the CO_2 system is often lacking (e.g., Jewett et al., 2020). Comparisons of observations further south in the California Current System have shown that upwelling water masses low in O_2 and high in CO_2 often influence nearshore ocean acidification and hypoxia (OAH) conditions (Chan et al., 2017; Kekuewa et al., 2022). However, freshwater influence is stronger in the northern California Current System and the Salish Sea, which can result in strong water column stratification and decoupling between shallow, nearshore and deeper conditions offshore. The Salish cruise data product provides the opportunity to develop empirical relationships for more localized areas of the southern Salish Sea and its boundary waters, including deeper parts of the water column (e.g., Juranek et al., 2009; Alin et al., 2012), to provide more relevant biogeochemical context for local ecosystem monitoring than offshore observations can provide.

Observations at the spacing of discrete samples were used to generate the depth transects in Figures 4–9. However, CTD cast data with higher vertical resolution (0.5 db bins) can be used as a basis for interpolating conditions between the more widely spaced discrete measurements presented in this article. High-resolution downcast CTD data corresponding to all oceanographic profiles in this data product are also publicly available (www.nanoos.org), but were not analyzed or archived at NCEI with the Salish cruise data product. For example, Reum et al. (2014) created high-resolution depth profiles of temperature, O_2, pCO_2, and Ω_{arag} conditions across 2008–2011 Salish cruises at stations in Hood Canal and Admiralty Reach using partial least squares regressions to interpolate conditions for each region and cruise. End users with needs for higher resolution water column information could use this interpolation approach based on combining the Salish cruise data product described here with downcast CTD data from the "Data" tab on the NANOOS Salish Cruise app (http://nvs.nanoos.org/CruiseSalish), which provides the downcast, high-resolution complement of the CTD parameters described in this article using upcast data at discrete sample spacing. Files on the NANOOS app also include data for potential temperature, oxygen saturation (%), chlorophyll fluorescence, beam transmission, beam attenuation, potentiometric pH for some cruises (on the NBS scale), and photosynthetically active radiation.

The data product can also inform biological assessments. Many regional species have inferred or known sensitivity to OA parameters (pCO_2 [partial pressure of CO_2], pH, Ω) (Busch and McElhany, 2016; Jones et al., 2018). The early part of this time-series was used to delineate the range of physical and biogeochemical conditions encountered by species of ecological or economic importance in the region (Reum et al., 2014, 2016). Pteropods, an exemplar of ocean acidification impacts, have been shown to

https://doi.org/10.5194/essd-2023-239
Preprint. Discussion started: 28 September 2023

experience pronounced dissolution in the Salish Sea, particularly in the more stratified and acidified basins (Bednaršek et al., 2021). Ongoing laboratory and field research to better understand the sensitivity of regionally important species (e.g., Miller et al., 2016; Bednaršek et al., 2020a, b, 2021, 2022; McElhany et al., 2022) has thus been able to use observed ranges and combinations of conditions encountered in the region for physical and OAH parameters rather than projections of future global ocean conditions that are often substantially inappropriate for representing the more dynamic and acidified coastal and estuarine ecosystems in Washington waters (Feely et al., 2008, 2016; Siedlecki et al., 2021).

An analysis of seasonal and interannual variability in the Salish cruise data product has provided preliminary information about the severity and relative frequency of ocean acidification, hypoxia, and marine heatwave conditions in the southern Salish Sea (Alin et al., 2023b). In combination with regional physical and oceanographic models (Khangaonkar et al., 2012; Siedlecki et al., 2016; MacCready et al., 2021), the Salish cruise data product can thus facilitate the extension of holistic vulnerability assessments like those that have been done for important shellfisheries on the coast (e.g., Hodgson et al., 2018; Berger et al., 2021) into Puget Sound, where the shellfish aquaculture industry contributed US$184M of economic activity, $77.1M of labor income, and 2710 jobs to the Washington state economy in 2010 (Northern Economics, Inc., 2013). Past studies have examined the distribution of Dungeness crab populations in Hood Canal, which are the target of valued regional tribal and recreational harvests, in response to hypoxia levels along the basin (Froehlich et al., 2014). The Salish cruise data product may facilitate a deeper look at whether crab populations respond to chronically acidified conditions in a similar way (Alin et al., 2023a, b), based on known responses to elevated CO_2 and decreased Ω and pH conditions as well the biological responses during their critical life stages (Miller et al., 2016; Bednaršek et al., 2020b; McElhany et al., 2022). Finally, the Salish cruise data product provides an important validation data set for the physical and biogeochemical parameters represented in the complex 3-D numerical simulations that to contribute to vulnerability assessments. Appropriate regional models operate on timescales from daily to seasonal forecasts (e.g., Siedlecki et al., 2015, 2016; MacCready et al., 2021) to multi-year hindcasts (Khangaonkar et al., 2021) or end-of-century projections (Khangaonkar et al., 2019; Bednaršek et al., 2020a; Siedlecki et al., 2021).

5.1.2 Potential future applications

The West Coast Ocean Data Portal is funding an effort to develop ocean indicators, including one to track ocean acidification status across the entire U.S. West Coast. Moored observations and numerical models allow the estimation of indicators such as the percent time or volume of water over which a location experiences conditions that surpass a given threshold (e.g., Sutton et al., 2016; Feely et al., 2023). Where estimates of preindustrial era CO_2 system conditions are available, they can provide a means of gauging the magnitude of change due to anthropogenic CO_2 versus natural processes or other anthropogenic causes (Sutton et al., 2016; Alin et al., 2023a). The Salish cruise data product offers the potential for creating seasonal OA indicators that estimate, e.g. the percent of the water column occupied by conditions that exceed a biological threshold. Another OA indicator could be the percent expansion of corrosive ($\Omega<1$) water since the preindustrial era within the more inland basins of the southern Salish Sea. Development of such indicators would further expand the applicability of Salish cruise data to the management of natural resources and water quality.

5.2 Data product limitations

The compiled Salish cruise data product provides observations from 35 cruises, each with coverage of at least part of the study region and providing spatial and depth sampling coverage not afforded by other platforms in inland waters. However, temporal resolution is at best seasonal, due to the expense and labor associated with conducting shipboard surveys. Thus, sampling of short-

https://doi.org/10.5194/essd-2023-239
Preprint. Discussion started: 28 September 2023

term events and illuminating the timeline of longer-lasting anomalies cannot be done solely with the Salish cruise data product. Fortunately, the region is also home to a number of time-series moorings that can be used to provide higher-resolution context for these detailed cruise observations at select locations through the study area (e.g., Northwest Environmental Moorings, https://nwem.apl.washington.edu/; and Olympic Coast National Marine Sanctuaries oceanographic moorings, https://olympiccoast.noaa.gov/science/oceanographic-moorings/). Multiple numerical models provide hindcasts and projections ocean physical and biogeochemical conditions on daily to end-of-century timescales in the region as well. Using a combination of oceanographic observations and models, end users of this data product may be able to fill gaps in spatial or depth coverage to fulfill diverse research objectives.

6 Conclusions

The Salish cruise data product provides a compiled data product including 35 cruise data sets that occupied stations in the southern Salish Sea and its boundary waters in the Strait of Juan de Fuca and nearby coastal waters obtained from 715 profiles of oceanographic data. This data product offers end users access to a decade of cruise time-series data with consistent formatting and both concentration and substance content units for commonly used parameters like oxygen and nutrients. Data from all cruises underwent added quality control measures, including extensive property-property plotting of biogeochemical and physical parameters, to identify and flag data points that may be anomalous. However, because the Salish Sea experienced a number of strong environmental anomalies during the 2008–2018 cruise time-series comprising the data product, anomalous data identified in this way were mostly flagged "questionable" rather than "bad" to allow end users to determine whether these data are ultimately suitable for their analyses. The Salish cruise data product presents climate-quality biogeochemical and physical oceanographic data from a productive, complex estuarine system with several basins with distinct water mass characteristics and dynamics. The data product thus assembles rich information that can be used to validate 3-D models of ocean conditions, frame biological sensitivity studies, and help end users and decision makers understand the range of conditions throughout the region and the dynamic interannual variability of ocean acidification and hypoxia here.

7 Data availability

All finalized data described in this publication can be accessed through the Ocean Carbon and Acidification Data Portal on the NOAA National Centers for Environmental Information web site (Alin et al., 2022; https://doi.org/10.25921/zgk5-ep63). After navigating to the HTTPS download link, the user can select one of the three data product versions described in Section 4.1 above. Filename "SalishCruise_dataProduct_2008to2018_09202023_CO2calcs.csv" contains the smallest subset of the data product, consisting of 3971 complete records of DIC, TA, T, S, O_2, and nutrient measurements with the highest quality QC flags, ready for calculations of the full carbonate system; this file is recommended for end users without strong familiarity with QCing or interpolating biogeochemical data. Filename "SalishCruise_dataProduct_2008to2018_09202023_questNut.csv" contains an additional 50 samples with nutrient data that require further QC attention (total of 4021 paired observations); all other data have "acceptable" QC flags. Filename "SalishCruise_dataProduct_2008to2018_09202023_allData.csv" contains the most complete version of the Salish cruise data product, including all data with "questionable" QC flags and data gaps for users with the capacity for or interest in interpolating to fill data gaps. An Excel file with updated metadata, including a tab detailing changes since the previous version of the data product on the NCEI page, is also available ("SalishCruise_dataProduct_2008to2018_metadata_09182023.xlsx"). The index of data product files for download can also be accessed via our NCEI landing page (https://www.ncei.noaa.gov/access/ocean-carbon-acidification-data-

https://doi.org/10.5194/essd-2023-239
Preprint. Discussion started: 28 September 2023

system/oceans/SalishCruise_DataPackage.html), which shows the map available for download on the HTTPS download page. Should users wish to download individual cruise data files or the original versions of each cruise submitted to NCEI, these are available in Table 1 at this landing page. To access the compiled data products from the landing page, the user would click the "Database Files" link to reach the index of data and metadata files associated with this data product (the same page reached via the HTTPS link described above). The data product files, along with a metadata file, a list of updates in more recent versions, and a standalone version of the map on the landing page can be downloaded by clicking on the relevant filename on the index webpage. End users are encouraged to use one of the compiled data sets described above, as these contain all updates to QC flags, and to always download and use the most recent version of each file.

Author contributions

SA led analysis of inorganic carbon samples, assembly and analysis of data and metadata, interpretation of data analyses, and manuscript drafting. JN led organization and execution of all cruises, oxygen and nutrient measurements, and provided input on data analysis and interpretations at all stages of the work. RF contributed to the development and implementation of this project and the writing of the manuscript. DG and BC performed significant data assembly, quality control, and management. DG prepared transect profile graphics. DG, BC, and JH contributed to data analysis and metadata preparation. MW and BC led CTD observations and data processing on several cruises each. All authors contributed to editing the manuscript.

Competing interests. The authors declare they have no competing interests.

Acknowledgments

We acknowledge that the land our laboratories are located on has been the home of Coast Salish people since time immemorial and that our study area encompasses the traditional and ancestral waters of the Coast Salish peoples and the Coastal Treaty Tribes of Washington. Several research and monitoring organizations have provided financial, logistical, and programmatic support for generating this time series of cruise observations in Washington marine waters; we are grateful for the leadership, support, and technical staff of the programs listed in Table 1. In particular, the Washington Ocean Acidification Center and NOAA's Ocean Acidification Program provided financial and logistical support that facilitated the stable sampling schedules in the latter part of the time series. We thank the officers and crew of all vessels in Table 1, as well as principal investigators who served on cruises but have not been involved with subsequent analyses, including John Mickett, Matt Alford, Jody Deming, and Carol Maloy. We are grateful to Corinne Bassin, Rachel (Vander Giessen) Wold, Marine LeBrec, Cynthia Peacock, Nancy Williams, Morgan Ostendorf (Langis), Alex Mitchell-Morton, and Paul Ruddell for their expertise in conducting the field work and laboratory analyses required to ensure consistently high-quality data for this cruise time-series. Li-Qing Jiang and Alex Kozyr of NOAA National Centers for Environmental Information provided invaluable assistance with data archival. This is PMEL contribution number 4700. This publication was partially funded by the Cooperative Institute for Climate, Ocean, & Ecosystem Studies (CICOES) under NOAA Cooperative Agreement NA20OAR4320271, Contribution No. 2023-1286.

References

Alin, S. R., Feely, R. A., Dickson, A. G., Hernández-Ayón, J. M., Juranek, L. W., Ohman, M. D., and Goericke, R.: Robust empirical relationships for estimating the carbonate system in the southern California Current System and application to CalCOFI hydrographic cruise data (2005–2011), J. Geophys. Res., 117, https://doi.org/10.1029/2011JC007511, 2012.

https://doi.org/10.5194/essd-2023-239
Preprint. Discussion started: 28 September 2023

Alin, S. R., Newton, J., Greeley, D., Curry, B., Herndon, J., Kozyr, A., and Feely, R. A.: A compiled data product of profile, discrete biogeochemical measurements from 35 individual cruise data sets collected from a variety of ships in the southern Salish Sea and northern California Current System (Washington state marine waters) from 2008-02-04 to 2018-10-19 (NCEI Accession 0238424), NOAA National Centers for Environmental Information, Dataset, https://doi.org/10.25921/zgk5-ep63, 2022.

Alin, S. R., Siedlecki, S. A., Berger, H., Feely, R. A., Waddell, J. E., Carter, B. R., Newton, J. A., Schumacker, E. J., and Ayres, D.: Evaluating the evolving ocean acidification risk to Dungeness crab: Time-series observations and modeling on the Olympic Coast, Washington, USA, Oceanography, https://doi.org/10.5670/oceanog.2023.216, 2023a.

Alin, S. R., Newton, J. A., Feely, R. A., Siedlecki, S., and Greeley, D.: Seasonality and response of ocean acidification and hypoxia to major environmental anomalies in the southern Salish Sea, North America (2014–2018), Biogeosciences Discussions, in review, 2023b.

Bakker, D. C. E., Pfeil, B., Landa, C. S., Metzl, N., O'Brien, K. M., Olsen, A., Smith, K., Cosca, C., Harasawa, S., Jones, S. D., Nakaoka, S., Nojiri, Y., Schuster, U., Steinhoff, T., Sweeney, C., Takahashi, T., Tilbrook, B., Wada, C., Wanninkhof, R., Alin, S. R., Balestrini, C. F., Barbero, L., Bates, N. R., Bianchi, A. A., Bonou, F., Boutin, J., Bozec, Y., Burger, E. F., Cai, W.-J., Castle, R. D., Chen, L., Chierici, M., Currie, K., Evans, W., Featherstone, C., Feely, R. A., Fransson, A., Goyet, C., Greenwood, N., Gregor, L., Hankin, S., Hardman-Mountford, N. J., Harlay, J., Hauck, J., Hoppema, M., Humphreys, M. P., Hunt, C. W., Huss, B., Ibánhez, J. S. P., Johannessen, T., Keeling, R., Kitidis, V., Körtzinger, A., Kozyr, A., Krasakopoulou, E., Kuwata, A., Landschützer, P., Lauvset, S. K., Lefèvre, N., Lo Monaco, C., Manke, A., Mathis, J. T., Merlivat, L., Millero, F. J., Monteiro, P. M. S., Munro, D. R., Murata, A., Newberger, T., Omar, A. M., Ono, T., Paterson, K., Pearce, D., Pierrot, D., Robbins, L. L., Saito, S., Salisbury, J., Schlitzer, R., Schneider, B., Schweitzer, R., Sieger, R., Skjelvan, I., Sullivan, K. F., Sutherland, S. C., Sutton, A. J., Tadokoro, K., Telszewski, M., Tuma, M., van Heuven, S. M. A. C., Vandemark, D., Ward, B., Watson, A. J., and Xu, S.: A multi-decade record of high-quality fCO_2 data in version 3 of the Surface Ocean CO_2 Atlas (SOCAT), Earth Syst. Sci. Data, 8, 383–413, https://doi.org/10.5194/essd-8-383-2016, 2016.

Banas, N. S., Conway-Cranos, L., Sutherland, D. A., MacCready, P., Kiffney, P., and Plummer, M.: Patterns of River Influence and Connectivity Among Subbasins of Puget Sound, with Application to Bacterial and Nutrient Loading, Estuaries and Coasts, 38, 735–753, https://doi.org/10.1007/s12237-014-9853-y, 2015.

Barnes, R. T. and Raymond, P. A.: The contribution of agricultural and urban activities to inorganic carbon fluxes within temperate watersheds, Chemical Geology, 266, 318–327, https://doi.org/10.1016/j.chemgeo.2009.06.018, 2009.

Bednaršek, N., Pelletier, G., Ahmed, A., and Feely, R. A.: Chemical Exposure Due to Anthropogenic Ocean Acidification Increases Risks for Estuarine Calcifiers in the Salish Sea: Biogeochemical Model Scenarios, Front. Mar. Sci., 7, 580, https://doi.org/10.3389/fmars.2020.00580, 2020a.

Bednaršek, N., Feely, R. A., Beck, M. W., Alin, S. R., Siedlecki, S. A., Calosi, P., Norton, E. L., Saenger, C., Štrus, J., Greeley, D., Nezlin, N. P., Roethler, M., and Spicer, J. I.: Exoskeleton dissolution with mechanoreceptor damage in larval Dungeness crab related to severity of present-day ocean acidification vertical gradients, Science of The Total Environment, 716, 136610, https://doi.org/10.1016/j.scitotenv.2020.136610, 2020b.

Bednaršek, N., Newton, J. A., Beck, M. W., Alin, S. R., Feely, R. A., Christman, N. R., and Klinger, T.: Severe biological effects under present-day estuarine acidification in the seasonally variable Salish Sea, Science of The Total Environment, 765, 142689, https://doi.org/10.1016/j.scitotenv.2020.142689, 2021.

Bednaršek, N., Beck, M. W., Pelletier, G., Applebaum, S. L., Feely, R. A., Butler, R., Byrne, M., Peabody, B., Davis, J., and Štrus, J.: Natural Analogues in pH Variability and Predictability across the Coastal Pacific Estuaries: Extrapolation of the Increased Oyster Dissolution under Increased pH Amplitude and Low Predictability Related to Ocean Acidification, Environ. Sci. Technol., 56, 9015–9028, https://doi.org/10.1021/acs.est.2c00010, 2022.

Benway, H., Alin, S., Boyer, E., Cai, W.-J., Coble, P., Cross, J., Friedrichs, M., Goñi, M., Griffith, P., Herrmann, M., Lohrenz, S., Mathis, J., McKinley, G., Najjar, R., Pilskaln, C., Siedlecki, S., and Smith, R.: A Science Plan for Carbon Cycle Research in North American Coastal WatersReport of the Coastal CARbon Synthesis (CCARS) community workshop, August 19-21, 2014, Ocean Carbon and Biogeochemistry Program and North American Carbon Program, 2016.

Berger, H. M., Siedlecki, S. A., Matassa, C. M., Alin, S. R., Kaplan, I. C., Hodgson, E. E., Pilcher, D. J., Norton, E. L., and Newton, J. A.: Seasonality and Life History Complexity Determine Vulnerability of Dungeness Crab to Multiple Climate Stressors, AGU Advances, 2, https://doi.org/10.1029/2021AV000456, 2021.

https://doi.org/10.5194/essd-2023-239
Preprint. Discussion started: 28 September 2023

Bianucci, L., Long, W., Khangaonkar, T., Pelletier, G., Ahmed, A., Mohamedali, T., Roberts, M., and Figueroa-Kaminsky, C.: Sensitivity of the regional ocean acidification and carbonate system in Puget Sound to ocean and freshwater inputs, Elementa: Science of the Anthropocene, 6, 22, https://doi.org/10.1525/elementa.151, 2018.

Busch, D. S. and McElhany, P.: Estimates of the Direct Effect of Seawater pH on the Survival Rate of Species Groups in the California Current Ecosystem, PLoS ONE, 11, e0160669, https://doi.org/10.1371/journal.pone.0160669, 2016.

Cai, W.-J., Feely, R. A., Testa, J. M., Li, M., Evans, W., Alin, S. R., Xu, Y.-Y., Pelletier, G., Ahmed, A., Greeley, D. J., Newton, J. A., and Bednaršek, N.: Natural and Anthropogenic Drivers of Acidification in Large Estuaries, Annu. Rev. Mar. Sci., 13, 23–55, https://doi.org/10.1146/annurev-marine-010419-011004, 2021.

Carpenter, J. H.: The accuracy of the Winkler method for dissolved oxygen analysis, Limnol. Oceanogr., 10, 135–140, https://doi.org/10.4319/lo.1965.10.1.0135, 1965.

Chan, F., Barth, J. A., Blanchette, C. A., Byrne, R. H., Chavez, F., Cheriton, O., Feely, R. A., Friederich, G., Gaylord, B., Gouhier, T., Hacker, S., Hill, T., Hofmann, G., McManus, M. A., Menge, B. A., Nielsen, K. J., Russell, A., Sanford, E., Sevadjian, J., and Washburn, L.: Persistent spatial structuring of coastal ocean acidification in the California Current System, Sci Rep, 7, 2526, https://doi.org/10.1038/s41598-017-02777-y, 2017.

Codispoti, L.: One man's advice on the determination of dissolved oxygen in seawater, 1988.

Dickson, A. G., Afghan, J. D., and Anderson, G. C.: Reference materials for oceanic CO2 analysis: A method for the certification of total alkalinity, Marine Chemistry, 80, 185–197, 2003.

Dickson, A. G., Sabine, C. L., Christian, J. R., Bargeron, C. P., and North Pacific Marine Science Organization (Eds.): Guide to best practices for ocean CO2 measurements, North Pacific Marine Science Organization, Sidney, BC, 1 pp., 2007.

Evans, W., Hales, B., and Strutton, P. G.: pCO_2 distributions and air–water CO_2 fluxes in the Columbia River estuary, Estuarine, Coastal and Shelf Science, 117, 260–272, https://doi.org/10.1016/j.ecss.2012.12.003, 2013.

Fassbender, A. J., Alin, S. R., Feely, R. A., Sutton, A. J., Newton, J. A., and Byrne, R. H.: Estimating Total Alkalinity in the Washington State Coastal Zone: Complexities and Surprising Utility for Ocean Acidification Research, Estuaries and Coasts, 40, 404–418, https://doi.org/10.1007/s12237-016-0168-z, 2017.

Fassbender, A. J., Alin, S. R., Feely, R. A., Sutton, A. J., Newton, J. A., Krembs, C., Bos, J., Keyzers, M., Devol, A., Ruef, W., and Pelletier, G.: Seasonal carbonate chemistry variability in marine surface waters of the US Pacific Northwest, Earth Syst. Sci. Data, 10, 1367–1401, https://doi.org/10.5194/essd-10-1367-2018, 2018.

Feely, R. A., Sabine, C. L., Lee, K., Berelson, W., Kleypas, J., Fabry, V. J., and Millero, F. J.: Impact of Anthropogenic CO_2 on the $CaCO_3$ System in the Oceans, Science, 305, 362–366, https://doi.org/10.1126/science.1097329, 2004.

Feely, R. A., Sabine, C. L., Hernandez-Ayon, J. M., Ianson, D., and Hales, B.: Evidence for Upwelling of Corrosive "Acidified" Water onto the Continental Shelf, Science, 320, 1490–1492, https://doi.org/10.1126/science.1155676, 2008.

Feely, R. A., Alin, S. R., Newton, J., Sabine, C. L., Warner, M., Devol, A., Krembs, C., and Maloy, C.: The combined effects of ocean acidification, mixing, and respiration on pH and carbonate saturation in an urbanized estuary, Estuarine, Coastal and Shelf Science, 88, 442–449, https://doi.org/10.1016/j.ecss.2010.05.004, 2010.

Feely, R. A., Alin, S. R., Carter, B., Bednaršek, N., Hales, B., Chan, F., Hill, T. M., Gaylord, B., Sanford, E., Byrne, R. H., Sabine, C. L., Greeley, D., and Juranek, L.: Chemical and biological impacts of ocean acidification along the west coast of North America, Estuarine, Coastal and Shelf Science, 183, 260–270, https://doi.org/10.1016/j.ecss.2016.08.043, 2016.

Feely, R. A., Carter, B. R., Alin, S. R., Bednaršek, N., and Greeley, D.: How anthropogenic carbon dioxide uptake and respiration reduce habitat suitability for marine calcifiers along the West Coast of North America, Journal of Geophysical Research: Oceans, 2023.

Froehlich, H. E., Essington, T. E., Beaudreau, A. H., and Levin, P. S.: Movement Patterns and Distributional Shifts of Dungeness Crab (*Metacarcinus magister*) and English Sole (*Parophrys vetulus*) During Seasonal Hypoxia, Estuaries and Coasts, 37, 449–460, https://doi.org/10.1007/s12237-013-9676-2, 2014.

https://doi.org/10.5194/essd-2023-239
Preprint. Discussion started: 28 September 2023

García, H. E. and Gordon, L. I.: Oxygen solubility in seawater: better fitting equations, Limnology and Oceanography, 37, 1307–1312, 1992.

Gattuso, J.-P., Epitalon, J.-M., Lavigne, H., Orr, J., Gentili, B., Hagens, M., Hofmann, A., Mueller, J.-D., Proye, A., Rae, J., and Soetaert, K.: Seawater carbonate chemistry. *R* Package "seacarb," 2022.

Hales, B., Suhrbier, A., Waldbusser, G. G., Feely, R. A., and Newton, J. A.: The Carbonate Chemistry of the "Fattening Line," Willapa Bay, 2011–2014, Estuaries and Coasts, 40, 173–186, https://doi.org/10.1007/s12237-016-0136-7, 2017.

van Heuven, S., Pierrot, D., Rae, J. W. B., Lewis, E., and Wallace, D.W.R.: MATLAB Program Developed for CO2 System Calculations. ORNL/CDIAC-105b. Carbon Dioxide Information Analysis Center, Oak Ridge National Laboratory, U.S. Department of Energy, Oak Ridge, Tennessee., 2011.

Hodgson, E. E., Kaplan, I. C., Marshall, K. N., Leonard, J., Essington, T. E., Busch, D. S., Fulton, E. A., Harvey, C. J., Hermann, A. J., and McElhany, P.: Consequences of spatially variable ocean acidification in the California Current: Lower pH drives strongest declines in benthic species in southern regions while greatest economic impacts occur in northern regions, Ecological Modelling, 383, 106–117, https://doi.org/10.1016/j.ecolmodel.2018.05.018, 2018.

Hunt, B. P. V., Alin, S. R., Bidlack, A., Diefenderfer, H., Jackson, J. M., Kellogg, C., Kiffney, P. M., St. Pierre, K., Carmack, E., Floyd, W. C., Hood, E., Horner-Devine, A. R., Levings, C., and Vargas, C. A.: Advancing an integrated understanding of land-ocean connections in shaping the marine ecosystems of Coastal Temperate Rainforest ecoregions (in review), Frontiers in Marine Science, 2023.

Ianson, D., Allen, S. E., Moore-Maley, B. L., Johannessen, S. C., and Macdonald, R. W.: Vulnerability of a semienclosed estuarine sea to ocean acidification in contrast with hypoxia, Geophysical Research Letters, 43, 5793–5801, https://doi.org/10.1002/2016GL068996, 2016.

IOC and SCOR: Protocols for the joint global ocean flux study (JGOFS) core measurements, Intergovernmental Oceanographic Commission and Scientific Committee on Oceanic Research, UNESCO, Paris, 1994.

IOC, SCOR, and IAPSO: The international thermodynamic equation of seawater – 2010: Calculation and use of thermodynamic properties, Intergovernmental Oceanographic Commission, UNESCO, 2010.

Jewett, E. B., Osborne, E. B., Arzayus, K. M., Osgood, K., DeAngelo, B. J., and Mintz, J. M.: NOAA Ocean, Coastal, and Great Lakes Acidification Research Plan: 2020–2029, 2020.

Jiang, L.-Q., Feely, R. A., Wanninkhof, R., Greeley, D., Barbero, L., Alin, S., Carter, B. R., Pierrot, D., Featherstone, C., Hooper, J., Melrose, C., Monacci, N., Sharp, J. D., Shellito, S., Xu, Y.-Y., Kozyr, A., Byrne, R. H., Cai, W.-J., Cross, J., Johnson, G. C., Hales, B., Langdon, C., Mathis, J., Salisbury, J., and Townsend, D. W.: Coastal Ocean Data Analysis Product in North America (CODAP-NA) – an internally consistent data product for discrete inorganic carbon, oxygen, and nutrients on the North American ocean margins, Earth Syst. Sci. Data, 13, 2777–2799, https://doi.org/10.5194/essd-13-2777-2021, 2021.

Jiang, L.-Q., Pierrot, D., Wanninkhof, R., Feely, R. A., Tilbrook, B., Alin, S., Barbero, L., Byrne, R. H., Carter, B. R., Dickson, A. G., Gattuso, J.-P., and Greeley, D.: Best Practice Data Standards for Discrete Chemical Oceanographic Observations, Frontiers in Marine Science, 8, 14, 2022.

Johannessen, S. C., Macdonald, R. W., and Paton, D. W.: A sediment and organic carbon budget for the greater Strait of Georgia, 16, 2003.

Johannessen, S. C., Macdonald, R. W., Burd, B., van Roodselaar, A., and Bertold, S.: Local environmental conditions determine the footprint of municipal effluent in coastal waters: A case study in the Strait of Georgia, British Columbia, Science of the Total Environment, 12, 2015.

Johnson, K. M.: Operator's manual: Single operator multiparameter metabolic analyzer (SOMMA) for total carbon dioxide (CT) with coulometric detection, Brookhaven National Laboratory, Brookhaven, N.Y., 1992.

Johnson, K. M., King, A. E., and Sieburth, J. M.: Coulometric DIC analyses for marine studies: An introduction., Marine Chemistry, 16, 61–82, 1985.

Johnson, K. M., Williams, P. J., Brandstrom, L., and Sieburth, J. M.: Coulometric total carbon analysis for marine studies: Automation and calibration., Marine Chemistry, 21, 117–133, 1987.

Johnson, K. M., Wills, K. D., Butler, D. B., Johnson, W. K., and Wong, C. S.: Coulometric total carbon dioxide analysis for marine studies: Maximizing the performance of an automated continuous gas extraction system and coulometric detector., Marine Chemistry, 44, 167–189, 1993.

Jones, J. M., Passow, U., and Fradkin, S. C.: Characterizing the vulnerability of intertidal organisms in Olympic National Park to ocean acidification, Elementa: Science of the Anthropocene, 6, 54, https://doi.org/10.1525/elementa.312, 2018.

Juranek, L. W., Feely, R. A., Peterson, W. T., Alin, S. R., Hales, B., Lee, K., Sabine, C. L., and Peterson, J.: A novel method for determination of aragonite saturation state on the continental shelf of central Oregon using multi-parameter relationships with hydrographic data, Geophys. Res. Lett., 36, L24601, https://doi.org/10.1029/2009GL040778, 2009.

Kekuewa, S. A. H., Courtney, T. A., Cyronak, T., and Andersson, A. J.: Seasonal nearshore ocean acidification and deoxygenation in the Southern California Bight, Sci Rep, 12, 17969, https://doi.org/10.1038/s41598-022-21831-y, 2022.

Khangaonkar, T., Sackmann, B., Long, W., Mohamedali, T., and Roberts, M.: Simulation of annual biogeochemical cycles of nutrient balance, phytoplankton bloom(s), and DO in Puget Sound using an unstructured grid model, Ocean Dynamics, 62, 1353–1379, https://doi.org/10.1007/s10236-012-0562-4, 2012.

Khangaonkar, T., Nugraha, A., Xu, W., and Balaguru, K.: Salish Sea Response to Global Climate Change, Sea Level Rise, and Future Nutrient Loads, J. Geophys. Res. Oceans, 124, 3876–3904, https://doi.org/10.1029/2018JC014670, 2019.

Khangaonkar, T., Nugraha, A., Yun, S. K., Premathilake, L., Keister, J. E., and Bos, J.: Propagation of the 2014–2016 Northeast Pacific Marine Heatwave Through the Salish Sea, Front. Mar. Sci., 8, 787604, https://doi.org/10.3389/fmars.2021.787604, 2021.

Lewis, E. and Wallace, D.: Program developed for CO_2 system calculations (CO2SYS), U.S. Department of Energy, Oak Ridge, Tennessee, USA, 1988.

MacCready, P., McCabe, R. M., Siedlecki, S. A., Lorenz, M., Giddings, S. N., Bos, J., Albertson, S., Banas, N. S., and Garnier, S.: Estuarine Circulation, Mixing, and Residence Times in the Salish Sea, Journal of Geophysical Research: Oceans, 126, e2020JC016738, https://doi.org/10.1029/2020JC016738, 2021.

McElhany, P., Busch, D. S., Lawrence, A., Maher, M., Perez, D., Reinhardt, E. M., Rovinski, K., and Tully, E. M.: Higher survival but smaller size of juvenile Dungeness crab (Metacarcinus magister) in high CO2, Journal of Experimental Marine Biology and Ecology, 555, 151781, https://doi.org/10.1016/j.jembe.2022.151781, 2022.

Miller, J. J., Maher, M., Bohaboy, E., Friedman, C. S., and McElhany, P.: Exposure to low pH reduces survival and delays development in early life stages of Dungeness crab (Cancer magister), Mar Biol, 163, 118, https://doi.org/10.1007/s00227-016-2883-1, 2016.

Moore, J., Bird, D. L., Dobbis, S. K., and Woodward, G.: Nonpoint Source Contributions Drive Elevated Major Ion and Dissolved Inorganic Carbon Concentrations in Urban Watersheds, Environ. Sci. Technol. Lett., 4, 198–204, https://doi.org/10.1021/acs.estlett.7b00096, 2017.

Moore-Maley, B. L., Ianson, D., and Allen, S. E.: The sensitivity of estuarine aragonite saturation state and pH to the carbonate chemistry of a freshet-dominated river, Biogeosciences, 15, 3743–3760, https://doi.org/10.5194/bg-15-3743-2018, 2018.

Newton, J., Feely, R., Jewett, E., Williamson, P., and Mathis, J.: Global Ocean Acidification Observing Network: Requirements and Governance Plan. Second edition, GOA-ON., 2015.

Northern Economics, Inc.: The economic impact of shellfish aquaculture in Washington, Oregon and California. Prepared for the Pacific Shellfish Institute., 2013.

Pacella, S. R., Brown, C. A., Waldbusser, G. G., Labiosa, R. G., and Hales, B.: Seagrass habitat metabolism increases short-term extremes and long-term offset of CO_2 under future ocean acidification, Proc. Natl. Acad. Sci. U.S.A., 115, 3870–3875, https://doi.org/10.1073/pnas.1703445115, 2018.

https://doi.org/10.5194/essd-2023-239
Preprint. Discussion started: 28 September 2023

Pelletier, G., Lewis, E., and Wallace, D.: CO2SYS.XLS: A calculator for the CO_2 system in seawater for Microsoft Excel/VBA, Wash. State Dept. of Ecology/Brookhaven Nat. Lab., Olympia, WA/Upton, NY, USA, 2007.

PSEMP Marine Waters Workgroup: Puget Sound marine waters: 2021 overview. J. Apple, R. Wold, K. Stark, J. Bos, P. Williams, N. Hamel, S. Yang, J. Selleck, S. K. Moore, J. Rice, S. Kantor, C. Krembs, G. Hannach, and J. Newton (Eds), https://www.psp.wa.gov/psmarinewatersoverview.php, 2022.

Reum, J. C. P., Alin, S. R., Feely, R. A., Newton, J., Warner, M., and McElhany, P.: Seasonal Carbonate Chemistry Covariation with Temperature, Oxygen, and Salinity in a Fjord Estuary: Implications for the Design of Ocean Acidification Experiments, PLoS ONE, 9, e89619, https://doi.org/10.1371/journal.pone.0089619, 2014.

Reum, J. C. P., Alin, S. R., Harvey, C. J., Bednaršek, N., Evans, W., Feely, R. A., Hales, B., Lucey, N., Mathis, J. T., McElhany, P., Newton, J., and Sabine, C. L.: Interpretation and design of ocean acidification experiments in upwelling systems in the context of carbonate chemistry co-variation with temperature and oxygen, ICES Journal of Marine Science, 73, 582–595, https://doi.org/10.1093/icesjms/fsu231, 2016.

Sabine, C. L., Feely, R. A., Gruber, N., Key, R. M., Lee, K., Bullister, J. L., Wanninkhof, R., Wong, C. S., Wallace, D. W. R., Tilbrook, B., Millero, F. J., Peng, T.-H., Kozyr, A., Ono, T., and Rios, A. F.: The Oceanic Sink for Anthropogenic CO_2, Science, 305, 367–371, https://doi.org/10.1126/science.1097403, 2004.

Sea-Bird Electronics: SBE 43 dissolved oxygen sensor – background information, deployment recommendations, and cleaning and storage, Sea-Bird Electronics, Bellevue, Washington, 2013.

Siedlecki, S. A., Banas, N. S., Davis, K. A., Giddings, S., Hickey, B. M., MacCready, P., Connolly, T., and Geier, S.: Seasonal and interannual oxygen variability on the Washington and Oregon continental shelves, J. Geophys. Res. Oceans, 120, 608–633, https://doi.org/10.1002/2014JC010254, 2015.

Siedlecki, S. A., Kaplan, I. C., Hermann, A. J., Nguyen, T. T., Bond, N. A., Newton, J. A., Williams, G. D., Peterson, W. T., Alin, S. R., and Feely, R. A.: Experiments with Seasonal Forecasts of ocean conditions for the Northern region of the California Current upwelling system, Sci Rep, 6, 27203, https://doi.org/10.1038/srep27203, 2016.

Siedlecki, S. A., Pilcher, D., Howard, E. M., Deutsch, C., MacCready, P., Norton, E. L., Frenzel, H., Newton, J., Feely, R. A., Alin, S. R., and Klinger, T.: Coastal processes modify projections of some climate-driven stressors in the California Current System, Biogeosciences, 18, 2871–2890, https://doi.org/10.5194/bg-18-2871-2021, 2021.

Sutton, A. J., Sabine, C. L., Feely, R. A., Cai, W.-J., Cronin, M. F., McPhaden, M. J., Morell, J. M., Newton, J. A., Noh, J.-H., Ólafsdóttir, S. R., Salisbury, J. E., Send, U., Vandemark, D. C., and Weller, R. A.: Using present-day observations to detect when anthropogenic change forces surface ocean carbonate chemistry outside preindustrial bounds, Biogeosciences, 13, 5065–5083, https://doi.org/10.5194/bg-13-5065-2016, 2016.

University of Washington: School of Oceanography Marine Chemistry Laboratory, https://www.ocean.washington.edu/story/Marine+Chemistry+Laboratory, last access: 20 June 2021.

Voss, B. M., Peucker-Ehrenbrink, B., Eglinton, T. I., Fiske, G., Wang, Z. A., Hoering, K. A., Montluçon, D. B., LeCroy, C., Pal, S., Marsh, S., Gillies, S. L., Janmaat, A., Bennett, M., Downey, B., Fanslau, J., Fraser, H., Macklam-Harron, G., Martinec, M., and Wiebe, B.: Tracing river chemistry in space and time: Dissolved inorganic constituents of the Fraser River, Canada, Geochimica et Cosmochimica Acta, 124, 283–308, https://doi.org/10.1016/j.gca.2013.09.006, 2014.

Wallace, R. B., Baumann, H., Grear, J. S., Aller, R. C., and Gobler, C. J.: Coastal ocean acidification: The other eutrophication problem, Estuarine, Coastal and Shelf Science, 148, 1–13, https://doi.org/10.1016/j.ecss.2014.05.027, 2014.

Wanninkhof, R.: Relationship between wind speed and gas exchange over the ocean revisited: Gas exchange and wind speed over the ocean, Limnol. Oceanogr. Methods, 12, 351–362, https://doi.org/10.4319/lom.2014.12.351, 2014.

Wilke, R., Wallace, D. W. R., and Johnson, K. M.: A water-based, gravimetric method for the determination of gas sampling loop volume, Analytical Chemistry, 65, 2403–2406, 1993.

Windham-Myers, L., Cai, W.-J., Alin, S., Andersson, A., Crosswell, J., Dunton, K. H., Hernandez-Ayon, J. M., Herrmann, M., Hinson, A. L., Hopkinson, C. S., Howard, J., Hu, X., Knox, S. H., Kroeger, K., Lagomasino, D., Megonigal, P., Najjar, R., Paulsen,

https://doi.org/10.5194/essd-2023-239
Preprint. Discussion started: 28 September 2023

M.-L., Peteet, D., Pidgeon, E., Schäfer, K., Tzortziou, M., Wang, Z. A., Watson, E. B., Cavallaro, N., Shrestha, G., Birdse, R., Mayes, M. A., Najjar, R., Reed, S., Romero-Lankao, P., and Zhu, Z.: Chapter 15: Tidal Wetlands and Estuaries. Second State of the Carbon Cycle Report, U.S. Global Change Research Program, https://doi.org/10.7930/SOCCR2.2018.Ch15, 2018.

WOCE: Chapter 4--Hydrographic Data Formats. In WHP Data Reporting Requirements (Rev. 2, February 1998), 1998.

955